A
Dissertation
on

"Synthesis and characterization of Niobium Carbide (NbC) Nano-powder"

Submitted in the fulfillment of the requirements for the award of degree of

Master of Technology
in
Metallurgical and Materials Engineering
(2013-2015)

submitted by

Aayush Gupta
(601302001)

under the guidance of

Dr. Om Prakash Pandey
(Senior Professor and Dean R & SP)

SCHOOL OF PHYSICS AND MATERIALS SCIENCE
THAPAR UNIVERSITY
PATIALA – 147004

July 2015

CERTIFICATE

This is to certify that this dissertation entitled **"Synthesis and Characterizations of Niobium Carbide (NbC) nano powder"** is submitted by **Mr. Aayush Gupta** (Roll. No. 601302001) in the fulfillment of the requirement for the award of degree of Master of Technology in Metallurgical and Materials Engineering from School of Physics and Materials Science, Thapar University, Patiala (Punjab), India. It is an exclusive record of candidate's own research under the supervision of **Dr. Om Prakash Pandey**. This dissertation in part or full has not been submitted in any other institution for the award of such kind of degree.

Dr. Om Prakash Pandey
(Supervisor)
Senior Professor and Dean R&SP
School of Physics and Materials Science
Thapar University, Patiala

Countersigned by:

Dr. M. K. Sharma
Professor & Head of Department
School of Physics and Materials Science,
Thapar University, Patiala

Dr. S. S. Bhatia
Dean of Academic Affairs
Thapar University, Patiala

ACKNOWLEDGMENT

I am submitting my dissertation for the fulfillment of my 'M. Tech.' degree. This work would not have been accomplished without the support, help and guidance of a large number of people. I express my deep gratitude and respect to my supervisor **Dr. O. P. Pandey** (Senior Professor, School of Physics and Materials Science) for his keen interest, strong motivation and constant encouragement during the course of the work. I thank him for his great patience, constructive criticism and myriad useful suggestions apart from invaluable guidance to me.

I would also like to thank **Dr. Kulvir Singh**, **Dr. Puneet Sharma**, **Dr. B. N. Chudasama** and all other faculty members of School of Physics and Materials Science for their constructive suggestions at different stages of this work.

The meaning of my life and work is incomplete without paying regards to my respected family whose blessings and continuous encouragement have shown me the path to achieve my goals. I would like to thank to **Mr. Gaurav Singla**, **Mr. Paramjyot Jha**, **Dr. Akshay Kumar**, **Mr. Devender Kumar**, **Ms. Loveleen Kaur Brar**, **Mr. Indermani Mishra**, **Savidh Khan**, **Nitin Gupta** and last but not the least **Mahesh Kumar Singh** for their patience, love, moral support and constant co-operation whenever I required.

And above all, I pay my regards to the Almighty for His blessings.

Aayush Gupta

ABSTRACT

Transition metal carbides are in demand for their unique properties resembling with metal and ceramic constituents. These carbides have high hardness, high melting temperature, and high-temperature strength. They have been used as hard constituents in metal matrix composites for high temperature applications and as coatings on cutting tools. Among these carbides, niobium carbide is a very important and promising example for industrial applications. Therefore in the present study niobium carbide (NbC) nanoparticles were synthesized through a reduction-carburization route by using niobium pentoxide and acetone (C_3H_6O) or charcoal as Nb and C sources along with metallic Mg as the reductant at 600 °C, 700 °C and 800 °C in an autoclave. The as-prepared NbC nanopowders were characterized and studied by X-ray powder diffraction, scanning electron microscopy and transmission electron microscopy at room temperature. The thermal stability of synthesized powder was investigated by differential thermal analysis and differential scanning calorimetry. The XRD results indicate that optimum reaction condition for the formation of nanocrystalline NbC was 600 °C for 2h carburization at high pressure with acetone and 800 °C for 10h with charcoal. The NbC nanoparticles produced from the present route typically have an average size around 90 nm (acetone) and 17 nm (charcoal) having core-shell structure. The influencing factors of the synthesis of the NbC nano powder have been discussed in present work.

List of Figures **Page**

List of Tables **Page**

Table of Content

1. Introduction

In 20th century, many of the scientists got fascinated by transition metals in industrial applications. Being an all-rounder material, transition metal compounds have been replacing the traditional components in various applications because of their excellent mechanical properties, high thermal stability, chemically inertness etc. Early transition metals (Group IV, V and VI) play crucial role among all the others metals of the d-block in periodic table. In the current situation of steel industries, these metals are being used as ferrite stabilizers due to their high affinity towards carbon. Their oxides, nitrides and carbides are being used as dispersed components to alter the thermal and wear stability of refractory components of aerospace industries as per requirement of application. While in machining industries transition metal carbides are employed as cutting tool materials. Besides this, their combination with hard metals (Co/WC-TiC,TaC) show better cutting efficiency which has revolutionized the machining industries and structural industry which have adopted this class of materials as its unified part. Instead of mechanical sectors, chemical and biotechnological industries are also overturned by their unreactive nature. Metal oxides and metal carbides have superseded the traditional platinum (Pt) in catalytic applications along with the very good photo-catalytic characteristics and non-toxicity of these classes of materials drew most of the bio-chemist's interest [1, 2].

Due to the continual minification of non-renewable energy sources, every conscious human is trying to increase the productivity either by reducing the amount or size. Reducing size was observed as the most appropriate criteria to enhance the desired properties. Scientists had succeed to minimize the size of materials to nano scale which has revolutionized all the application sectors from mass production of giant machinery to doping of element at atomic level to modify the electronic characteristics. Thin film of carbide improves the mechanical properties of substrate component drastically while dispersion of such tiny particles alters the base alloy's characteristics. For example in automotive industries, the piston alloys are reinforced by tungsten

carbide, titanium carbide, alumina etc. which enhances the thermal, fatigue strength. Even at nano scale transition metal carbides and oxides are very promising materials. They are being used in fuel cells to store energy, to store gas by adsorption, act as catalyst to promote the chemical reaction in the desired direction and to degrade the bio-compatible dyes under the exposure of specific electromagnetic radiation [3, 4]. Only because of the drastic variation of properties by reducing the size of materials, every researcher is working to modify the structures which results very high degree of improvement in properties for better applications. Under the consideration of such applications such class is very important to study; how their production and application can be modified to intensify the industrial revolution.

1.1. Transition Metal Carbides (TMCs):

The applications of TMCs have been known for over one hundred years. Titanium carbide (TiC) and tungsten carbides (WC) were extracted from steel and properly identified around the middle of the 19^{th} century. Titanium carbide was first described in 1822 and identified by chemical analysis in 1850. The industrial importance of the refractory carbides is growing rapidly, not only in the traditional and well-established applications based on the strength and refractory nature of these materials such as cutting tools and abrasives, but also in new and promising fields such as electronics and catalysis. Some typical applications are as follows:

- Tungsten carbide (WC) and Titanium carbide (TiC) cutting tools.
- TMCs can be used as efficient and abundant electro-catalysts for the production of hydrogen that minimizes energy consumption [5].
- Cemented Carbides like WC-(Ti,W)C, WC-(W,Ti,Ta,Nb)C etc. can be used in mining, construction, rock drilling, metal forming and structural components [6].

Such a wide range of applications reflect the variety of these materials and the diversity of the industry, from small research laboratories developing new ideas to large plants manufacturing cutting tools, textile machinery, electronics and semiconductor components, and many other

products. Together, these organizations form an essential part of the ceramic industry throughout the world. Because of their great strength and durability, they have traditionally been used at extreme conditions of temperature and pressure; for example, in rocket nozzles and drill bits. Their hardness has given them applications in cutting tools, golf shoe spikes, and snow tires. In ferrous alloys they are the components responsible for the toughness of steels. However, they also have interesting optical, electronic, and magnetic properties and have been used for optical coatings, electrical contacts, diffusion barriers.

The word *'refractory'* defines a material having a high melting point. In this context, it designates any carbide with a melting point arbitrarily selected as greater than 1800°C. To be considered as refractory, the material must have a high degree of chemical stability.

Most elements form carbides which can be divided into several categories with different physico-chemical structures and characteristics. Among all of these, however, only the interstitial and covalent materials meet the refractory qualification. This includes the carbides of the nine transition elements of groups IV, V, and VI. Although, carbides as a group form the most refractory compounds that are certainly not the only ones. Several nitrides, borides, oxides, phosphides, silicides, and metals meet the refractory requirements.

Definition: The carbon forms compound with most of the other elements in periodic table but the term 'carbide' is used for those compound in which carbon is bonded with lower or equal (nearly) electro-negativity. This branch of compounds can be classified on the basis of the nature of bond between carbon and other element, which are as follows:

1.1.1. Salt like carbide (Group I, II and III)

This class of carbide compounds can be referred as salinic materials. The bond formation takes place between carbon and the most electropositive elements of the periodic table with the electronegativity difference of about 2 or more and these molecules have at least 50% ionic character. They form transparent and colorless crystals. Some contain C^{4-} ions such as aluminum

carbide (Al_4C_3) and beryllium carbide (Be_2C). They evolve methane when hydrolyzed and for that reason are usually known as methanides. Others contain C^{2-} ions such as calcium carbide (CaC_2); they yield acetylene when hydrolyzed and are known as acetylides [6, 7].

1.1.2. Interstitial carbide (Group IV, V and VI)

The difference in electronegativity between the two elements of the interstitial carbides is large. The carbon atom has a much smaller size than the other atom, allowing it to nest in the interstices of the lattice (hence the name interstitial). The bonding is partly covalent and ionic, but mostly metallic which explains why the interstitial carbides closely resemble metals. Like metallic alloys, their composition is often indeterminate and their electrical and thermal conductivities are high. In addition, they have high melting points, high hardness and are chemically inert [7].

1.1.3. Covalent carbide (Boron, Silicon)

The difference in electronegativity between the two elements of the covalent carbides is small. The carbon atom is only slightly smaller than the other atom. The bonding is essentially covalent [7]. Only two covalent carbides, silicon carbide and boron carbide, fully meet the refractory criteria. Other carbides such as beryllium carbide, Be_2C are only partially covalent and, while they have a high melting point, are generally not chemically stable.

1.1.4. Intermediate carbide (Group VII, VIII)

Some transition metals of groups VII and VIII such as manganese (Mn), iron (Fe), cobalt (Co), and nickel (Ni), as well as chromium (Cr) of group VI also form carbides but, their atomic radii are too small to accommodate the carbon atom in interstitial positions without severe distortion of the lattice. The carbon atoms are close enough for carbon-carbon bonds and carbon chains to form [7]. These carbides are not generally chemically stable. They are hydrolyzed by water or by dilute acids to produce hydrocarbons and hydrogen. An exception is chromium carbide, Cr_3C_2, which is a refractory border-line case.

1.2. General Characteristics of Interstitial Carbides

These are the crystalline compounds made of a metal, belongs to d-block (specially group IV, V, VI) and carbon. Generally, the metal is closely packed and carbon attains specific interstitial sites in that structure. This model restricts the occupancy of site by the carbon atom at all the available interstitial sites determines the stoichiometry of the crystal. Such interstitial structure was empirically formulated by Hägg in 1931, hence referred as 'Hägg's structure'. He observed that 9 early transitions metals are fit for these criteria of size and site availability which are as follows:

Table 1: Transition metals of group IV, V and VI.

	Group IV	**Group V**	**Group VI**
4th period	Titanium (Ti)	Vanadium (V)	Chromium (Cr)
5th period	Zirconium (Zr)	Niobium (Nb)	Molybdenum (Mo)
6th period	Hafnium (Hf)	Tantalum (Ta)	Tungsten (W)

The atomic structure of interstitial carbides is a mixture of ionic, covalent, and metallic bonding. As a result, the properties of these compounds reflect this structural mix and combine metallic and ceramic characteristics as summarized as follows:

1) Metallic bonding (metal-like properties)
    i) High thermal conductivity
    ii) High electrical conductivity
    iii) Sequence of distinct phases
2) Covalent bonding (ceramic-like properties)
    i) High hardness
    ii) High bond strength and brittleness
    iii) Very high melting point and refractoriness
3) Ionic bonding
    i) Chemical behavior of ionic crystals

ii) High electron energy level

All the interstitial carbides have many characteristics in common:

1) They fully meet the refractory criteria.
2) They are primarily non-stoichiometric phases.
3) They have high thermal and chemical stability.
4) Group IV, V and VI metal carbides possess good mutual solubility [8, 9], some of them are complete soluble, some show partial solubility and very few elements are insoluble.

1.3. Crystal structure and composition

The crystal structures of the carbides display considerable variation. In the left side of d-block i.e. group III-V; the structures tend to be simple, very often resembling those of the pure transition metals themselves. However, beyond the group VI in the periodic table, or in compositions involving electropositive elements (e.g. groups I or II), the structures adopted tend to be more complicated. These trends were first systematized by Hägg's rule [10], which states that *the structure formed depends on the radius ratio* $R = r_c/r_m$, where r_c and r_m are the radii of the nonmetal (carbon) and metal atoms, respectively. When 'R' is less than 0.59, the transition metals form the common structures: face-centered cubic (fcc), hexagonal closed packed (hcp) or simple hexagonal, with the nonmetal atoms placed in the large interstitial sites of octahedral or cubic prismatic geometry. When 'R' is greater than 0.59, the metallic arrangement distorts to accommodate the larger non-metal atoms and to preserve metal-metal interactions. The effect of electronic structure is reflected in systematic crystal structure changes in the metals, and in the carbides. Although the parent metals are body centered cubic (bcc), in carbides the metallic arrangement is cubic (fcc) or hexagonal (figure 1).The shift in structure correlates with the number of valence electrons in carbon and suggests that these elements increase the concentration of sp electrons in the alloys. The group III-V compounds follows these trends. However, because of their MX stoichiometry, they have a high non-metal content and high sp

electron density, an fcc arrangement of metal atoms is observed. Group VI-VIII compounds, which show increasingly complex structures compared to the group III-V compounds. Whereas in the early transition metals (group III-V) the formulas MX and M_2X are prevalent, in the later transition metals (group VI-VIII), the stoichiometry shifts to M_3X and M_4X. For the metals a maximum in melting point is observed between groups V and VI, while for the carbides the maximum is shifted to group V. The shift in the carbides towards group V correlates with the number of valence electrons in carbon and suggests a greater degree of band-filling in the compounds.

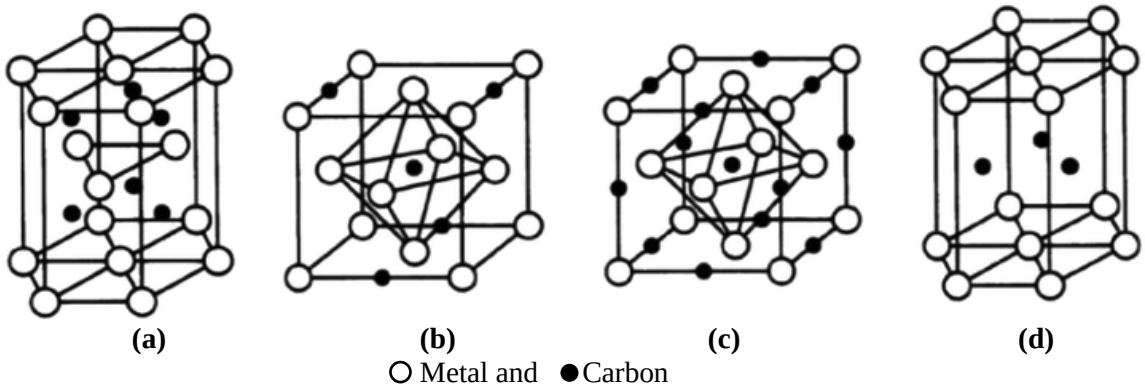

Figure 1: Crystal structures of transition metal carbide (a) hcp (WC); (b) fcc (Mo_2C); (c) fcc (NbC, VC, TaC) and (d) simple hexagonal (Cr_3C_2).

1.4. Physical Properties

1.4.1. Melting point

The spectacular property of transition metal carbides is their very high melting point. Several carbides melt or decompose above 3000 °C and TaC has the highest melting point [11, 12]. In transition metals, group VI elements have the highest melting point; while in the case of carbides, the maxima lies in group V. The most considerable feature is the variation of melting point during the transition from pure metal to the respective carbide. The differences are smaller for those of group V elements, while in group VI the reverse occurs as the metals have higher melting points than the corresponding carbides. The higher melting point of carbides which are reflected by the high bonding energies of metal-carbon bonds (groups IV and V) [11].

1.4.2. Density

All the metals of group V and VI have body centered cubic (bcc) crystal structure while Ti and Zr of group IV have hexagonal closed packed (hcp) structure. During the carburization of all the metals, most of these transform their structure to face centered cubic (fcc) structure from bcc structure due to which all the carbides show negative deviation in density from their respective metallic structure. While TiC and ZrC both have higher density than their respective metals corresponding to a larger increase in metal to metal spacing occurring during formation of the mono-carbide [11-14].

1.4.3. Heat of Formation

Properties such as heat of formation and standard entropy are important factors in determining the bonding nature of carbides [15]. Within each group, the absolute values of heat of formation are relatively close but decrease noticeably when going from group IV to group VI. These characteristics of the heat of formation show the greater stability of the carbides of group IV which would imply that the bonding portions of their electron band structure are filled (i.e., a half-filled d-shell). The carbides of group V and especially those of group VI are less stable which may be related to the gradual filling of the anti-bonding portion of the bond [13].

1.5. Thermal Properties

1.5.1. Thermal Conductivity

The thermal conductivity of interstitial carbides is different from that of most of other refractory materials which increases with the increasing in temperature [16]. Typically, the mechanism of thermal conductivity involves two components: electron thermal conductivity and phonon (lattice) conductivity. The thermal conductivity increases markedly with temperature. This behavior is believed to be the result of strong scattering of electrons and phonons by carbon vacancies in addition to the scattering of electrons by polar optical phonons and the scattering of phonons by the conduction electrons. Among all the metal carbides WC (63.0 W/m-K) and NbC

(14.2 W/m-K) show the highest and lowest magnitude of thermal conductivities respectively [11].

1.5.2. Thermal Expansion

The interatomic spacing between the atoms of a carbide (as with any other material) is a function of temperature. At zero degree K (-273 °C) these atoms have their lowest energy position, they are in the ground state. The increased energy resulting from increasing temperature causes the atoms to vibrate and move farther apart. In other words, the mean interatomic spacing increases and the result is thermal expansion. In strongly bonded carbides, the amplitude of the vibrations is small and the dimensional changes remain small. The thermal expansion increases with increasing temperature but this increase is not linear and is slightly more rapid at high temperature [16].

1.6. Electrical Resistivity

Materials can be classified as conductors, semiconductors or insulators. Conductors typically have resistivity in the range 10^{-2}-10^{3} μΩ-cm, semiconductors 10^{6}-10^{11} μΩ-cm, and insulators about 10^{13}-10^{18} μΩ-cm. Although the carbides have somewhat higher resistivity than the pure metals, they still have resistivity in the regime of conductors. WC and TaC own minimum (~22 μΩ-cm) among all of the 9 metal carbides while Cr_3C_2 and TiC possess maximum (~68 μΩ-cm). Rests of all metal carbides have their electrical resistivity in the order of 35-60 μΩ-cm [6].

1.7. Mechanical properties

The mechanical properties of transition-metal carbides are reviewed in detail by Toth [14]. Mechanical properties are referred as the response of a material under the application of forces. These forces can be of different types like longitudinal, transverse and fluctuating forces etc. The responses towards these external or internal forces are termed as yield strength, shear strength, hardness, toughness etc. These mechanical properties depend on some parameters of material which are enlisted as follows [17, 18]:

1) Stoichiometry
2) Impurities particularly oxygen and nitrogen
3) Grain size and morphology
4) Structural defects (vacancies, dislocations)
5) Presence of different phase

The mechanical properties of cermet (multi metallic carbides) are often quite different from those of single crystal or polycrystalline materials [19]. Hardness involves elastic and plastic deformation, crack initiation, and the development of new surfaces. Group IV carbides have higher hardness than those of groups V and VI which results to their better stability. Another property is stiffness which is termed as stress required inducing unit elastic strain by changing sample's length. More precisely, it is referred as young's modulus. Speck and Miccioli studied the temperature and porosity dependence of the elastic modulus of hot pressed NbC and showed that in the temperature range of 273-1870 K, both the Young's modulus and the shear modulus decrease by 25%; the elastic modulus also decreased by 20% with 10% porosity in the sample [20]. From all of the above properties we can say TMCs have high hardness, good thermal and electrical conductivities which account for the wear resistant applications as their major importance. This can be achieved by providing TMCs coating on different substrates by vapor deposition techniques, flame spraying and plasma jets etc.

For machining purposes, WC-Co tools with 3-12 wt% Co and carbide grain sizes from 0.5 to ~5 μm are commonly used. These straight (non-alloyed) WC-Co materials have excellent resistance to simple abrasive wear and are widely used in machining materials that produce short chips, e.g. gray cast-iron, nonferrous alloys, high temperature alloys, etc. Straight WC-Co tools are not suitable for machining steels that produce long chips because straight grades undergo crater wear from diffusion of WC into the steel chip surface. However, solid solutions of WC-TiC, WC-TiC-TaC etc. resist this type of chemical attack and steel cutting compositions typically contain WC-

(W,Ti,Ta,Nb)C-Co. The performance of cemented carbide tools is determined not only by chemical composition (amount of carbides and binder metal), but by the size and distribution of WC, solid solution carbides, and the binder in their microstructures. These in turn determine the physical and mechanical properties of the tools [21].

1.8. Chemical Property: Electro-catalytic activity

It has been established that early transition (groups IV-VI) metal carbides (TMCs) often share similar electronic and catalytic properties with the Pt-group metals [22] and can be used as supports to reduce the overall loading of the precious metals. Fuel cells and electrolyzers typically require the use of significant amounts of precious metals, such as platinum (Pt), palladium (Pd) which greatly increases the cost of these devices. An ultralow loading of one monolayer (ML) of Pt can be stable on several TMC supports while behaving as active as bulk Pt for the hydrogen evolution reaction (HER) [23, 24]. Tungsten carbide (WC) has been studied extensively as both a stand-alone electrocatalyst and as a support for Pt-group metals for the HER [25, 26], hydrogen oxidation reaction (HOR) [27], methanol oxidation reaction [28], and oxygen reduction reaction (ORR) [29]. The performance of the TMCs was compared with transition metal nitrides, sulfides, silicides, and borides with Pt as benchmark. The HER overpotential has been a common way to describe activity. A three-dimensional plot of the overpotential as a function of transition metal and their refractory compounds is presented in Figure 2.

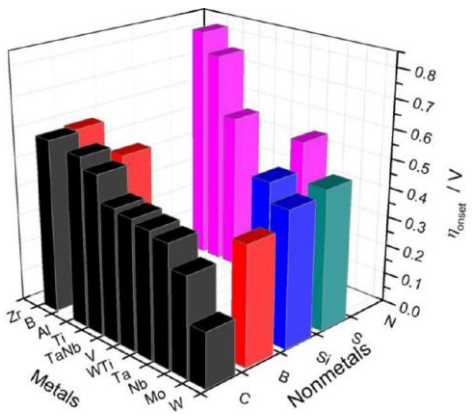

Figure 2: 3D plot of the over-potential for the hydrogen evolution reaction at the studied refractory ceramics as a function of their components. Low columns represent a high performance; high column represent low catalytic activity. [©30].

Although every transition metal carbide show refractory character on its own and very good mechanical properties, some of them are very critical compounds such as WC, NbC and TiC. From the family of carbides niobium carbide is a crucial member to study which contains very good toughness, least thermal conductivity with excellent non-reactive nature in chemical environment. Various physical, mechanical, thermal and electrical properties of NbC are enlisted as follows:

Table 2: Comparison among different TMCs as per their properties.

Property	Tungsten Carbide (WC)	Tantalum Carbide (TaC)	Vanadium Carbide (VC)	Niobium Carbide (NbC)
Crystal Structure	hexagonal	fcc	Fcc	**fcc**
Melting Point (°C)	2870	3950	2830	**3600**
Density (gm/cm^3)	15.8	14.5	5.65	**7.79**
Coefficient of Thermal Expansion ($\times 10^{-6}$/°C)	7.3	6.3	7.2	**6.6**
Heat of Formation (KJ/mole)	40.55	142.67	102.51	**140.58**
Young's modulus (GPa)	620-720	285-560	430	**340-580**
Vicker's Hardness (GPa)	22.0	16.7	27.2	**19.6**
Electrical resistivity (μΩ-cm)	22	25	60	**35**
Thermal Conductivity (W/m-K)	63..0	22.1	38.9	**14.2**

1.9. Niobium-Carbon (Nb-C) system:

The study on the synthesis of NbC was carried by Joly in 1877 from the reaction of $K_2O.3Nb_2O_5$ and carbon which is the earliest reported information [31]. Basically at that time Nb_2O_5 was the common choice for the researchers but in the present time it is being used for industrial production of carbide. After Joly's work, many scientists had worked on NbC by changing the source of niobium and mode of reaction. All of them concluded that it is a high temperature process which requires very high amount of energy to form Nb-C bond in solid state and it can be

reduced by changing the reactant's phase or by making an intermediate compound to result NbC after heat treatment. The reaction between Nb_2O_5 and carbon starts from 675 °C (Elyutin et al. 1958) [32]. Below 1200 °C lower oxides and NbC_x were the major products of the reaction while further increase in temperature to 1500 °C leads to form NbC_xO_y solid solution. Further higher temperature tends to form Nb metal. Some authors studied this behavior and suggested that the rise in temperature at first favors the reaction to form NbC, but at higher temperature and appropriate stoichiometry, Nb metal is formed (Shveikin 1958, Kusenko and Gel'd 1961) [33, 34]. Collectively it can be concluded that to form Nb-C bond it is necessary to eliminate oxygen from the crystal which was initially done by heating (Nb_2O_5 + C) in vacuum above 1900°C. This phenomenon was quite time consuming. Storms and Krikorian 1960 suggested using H_2 atmosphere to reduce the duration. The bond formation between Nb and C can be studied by using their phase diagram which provides almost all the combinations of Nb and C with respect to temperature and alloy content. As shown in figure 3 (Nb-C phase diagram), two major compounds are formed: Nb_2C and NbC. Pure niobium metal has melting point of 2469 °C and Nb-C system shows eutectic behavior at ~10.5% of carbon at 2340 °C which was supported by Pochon et al. [35], Elliot (1959) [36] , Kimura and Sasaki (1961) [37] and 3350 °C at ~60% of carbon. The solubility of carbon in Nb metal is around 0.8% at 1500 °C and Nb_2C phase also possess very narrow range of existence at low temperature. NbC phase exists from $NbC_{0.7}$ to $NbC_{0.99}$ and as the molar ratio approached to 1:1, the reaction becomes increasingly slow. If Nb metal is soluble in graphite, this limit is less than 0.01% after being cooled rapidly from the melt.

1.10. Various properties of Niobium Carbide:

1.10.1. Lattice Parameter and Density: Lattice parameter of carbide materials majorly depends on the diffusion of carbon into metal lattice. Many researchers proposed various trends of lattice constant, the most commonly used relation for the lattice parameter of NbC based on the composition is as follows

$$a_0 = 4.09847 + 0.7182\,(C/Nb) - 0.3457\,(C/Nb)^2 \quad \textbf{(i)}$$

where C/Nb is atom ratio [39]. Based on the above equation, the density of crystal decreases to 7.71 gm/cm^3 from 7.78 gm/cm^3 as the carbon content decreases from $NbC_{0.99}$ to $NbC_{0.78}$ and again rises to 7.73 gm/cm^3 at NbC-Nb_2C phase boundary.

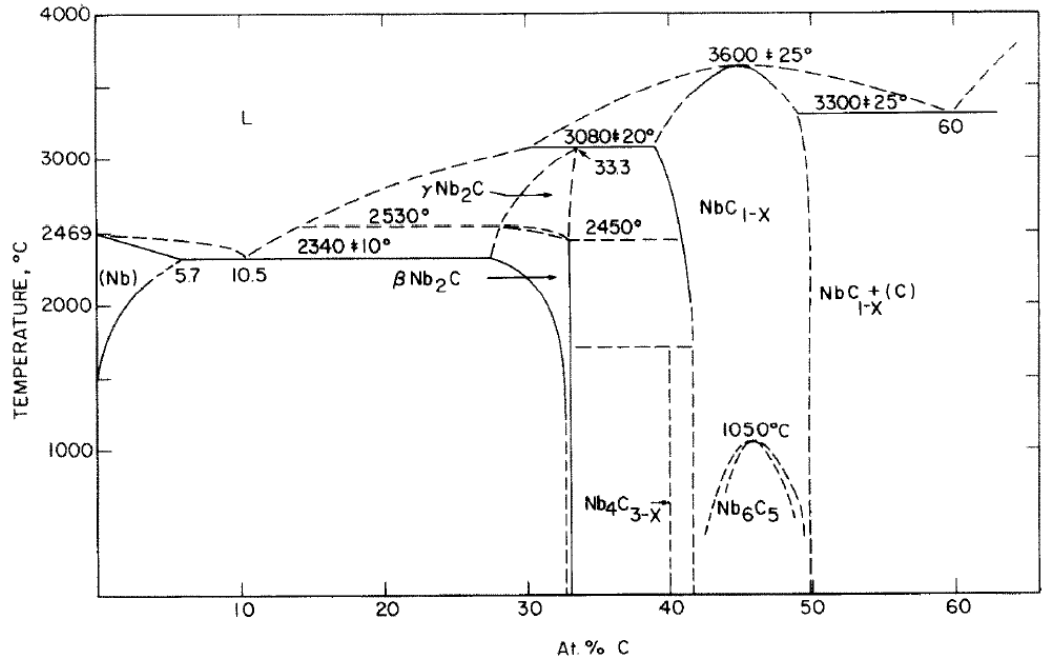

Figure 3: Phase diagram of Nb-C system [38].

1.10.2. Chemical Reactivity: NbC is extremely unreactive; even boiling in aqua regia does not attack the carbide powder. A solution of HNO_3 and HF is needed for dissolution to occur. NbC tends to burn when heated in oxygen and above 1100 °C corrosion becomes severe [40].

1.10.3. Thermochemical Properties: Several scientists have worked to calculate the heat of formation of NbC. The heat of formation of Nb_2O_5 and CO_2 is -455.2 kcal/mole and -94.05 kcal/mole respectively. These calculations were made under the assumption of constant pressure, effect of impurities. The proposed dependence of heat of formation on the carbon content can be expressed as

$$\Delta H_f\,(293.15K, kcal/mole) = 6.6 - 70.95\,(C/Nb) + 30.75\,(C/Nb)^2$$

Where C/Nb is atom ratio [41]. They obtained -23.3±0.6 kcal/mole for Nb_2C and -4±0.6 kcal/mole for $NbC_{0.98}$. The values 8.81 cal/mole-K and 8.46 cal/mole-K at 298.15 K as heat

capacity and entropy respectively were suggested for $NbC_{0.99}$. The heat of formation (cal/mole) of $NbC_{0.98}$ as a function of temperature can be expressed as [40, 42]

$$\mathbf{H_T - H_{298.15} = -4.0918\times10^3 + 10.8561(T) + 9.174\times10^{-4}(T^2) - 5.2003\times10^{-8}(T^3) + 2.3105\times10^5(T^{-1})}$$

1.11. Advantages of Niobium carbide over other TMCs:

Niobium Carbide (NbC) is a very important among all TMCs because of its very good thermal stability and better toughness. NbC possess least hardness among rest of all TMCs, which makes it very suitable material for reinforcing in various alloys such as austenitic steel, martensitic steel, cast iron and various cermets etc. In aerospace applications (cryogenic), addition of NbC to steel leads to enhance its formability and corrosion as compared to other TMCs like tungsten carbide (WC), tantalum carbide (TaC) and chromium carbide (Cr_3C_2). The most importantly niobium possess similar properties to tantalum with lower weight density which makes it very critical element for aerospace industry (more precisely) to enhance strength to weight ratio of an aircraft. Except these, NbC is very much competitive to other TMCs in wear applications; from literature it is clear that it shows lower wear rate under dry sliding application as compared to bearing steel. Addition of NbC in cermets improves their fracture toughness which can be used in different sectors like heating elements in resistance furnaces and doping of NbC in WC-(W,Ti,Ta,Nb)C-Co enhances the cutting tool life.

Electro-catalytically NbC shows better results for hydrogen evolution reaction except WC and Mo_2C, which may make it as an alternative material for low cost hydrogen evolution catalysis. Due to poor stability at higher temperature in any electrolytic environment, it captures a good position in low temperature fuel cell application. On the basis of above reasons, the synthesis and application study of NbC becomes very crucial.

1.12. References:

[1] F. Harnisch, G. Sievers and U. Schroder, **Tungsten carbide as electrocatalyst for the hydrogen evolution reaction in pH neutral electrolyte solutions**, Applied Catalysis B: Environmental 89, 455 (2009).

[2] H. Zheng, J. Huang, W. Wang and C. Ma, **Preparation of nano-crystalline tungsten carbide thin film electrode and its electrocatalytic activity for hydrogen evolution**, Electrochemistry Communications 7, 1045 (2005).

[3] D.J. Ham and J.S. Lee, **Transition metal carbides and nitrides as electrode materials for low temperature fuel cells**, Energies 2, 873 (2009).

[4] Y. Chen, H. Zhang, J. Zhang, J. Ma, L. Wangd, H. Ye, G. Qian andY. Ye, **Facile synthesis, characterization and photocatalytic activity of niobium carbide**, Advanced Powder Technology 24, 207 (2013).

[5] W.F. Chen, J.T. Muckerman and E. Fujita, **Recent developments in transition metal carbides and nitrides as hydrogen evolution electrocatalysts**, Chem. Commun. 49, 8896 (2013).

[6] S.T. Oyama, **The chemistry of transition metal carbides and nitrides**, Blackie Academic and Professional, Glasgow (1996).

[7] F.A. Cotton, and G. Wilkinson, **Advanced inorganic chemistry**, Inter-science Publishers, New York (1972).

[8] H. Holleck, **Material selection for hard coatings**, J. Vuc. Sci. Technol. A 4(6) (1986).

[9] H. Tulhoff, Carbides, **Ullmann S encyclopedia of industrial chemistry**, 5th. Ed., Vol. 15, VCH (1985).

[10] G. Hagg., Z. Phys. Chem., 12, 33 (1931).

[11] T.Y. Kosolapova, **Carbides: properties, production and applications**, Plenum Press, NewYork-London (1971).

[12] I.E. Campbell and E.M. Sherwood, **High-temperature materials and technology**, John Wiley & Sons, New York (1967).

[13] E.K. Storms, **The refractory metal carbides**, Academic Press, New York (1967).

[14] L.E. Toth, **Transition metal carbides and nitrides**, Academic Press, New York (1971).

[15] A.F. Guillermet and G. Grimvall, **Cohesive properties and vibrational entropy of 3d-transition metal carbides**, J. Phys. Chem. Solids 53(1), 105 (1992).

[16] **Engineering property data on selected ceramics**, Vol. 2, Carbides, MCIC HB-07-2, Battelle Institute, Columbus, OH (1987).

[17] Y. Ishizawa and T. Tanaka**, Fermi surface properties and bonding nature of TiB_2 and WC,** Science of hard materials, Institute of Physics Conf. 75, Adam Hilger Ltd. Bristol, UK (1984).

[18] J.E. Sundgren, B.O. Johansson, A. Rockett, S.A. Barnett and J.E. Greene, **TiN atomic arrangement, electronic structure and recent results on crystal growth and physical properties of epitaxial layer**, AIP Conference Proceedings 149, 95 (1986).

[19] V.K. Sarin**, Cemented carbide cutting tools**, Advances in Powder Technology, (G, Y. Chin. ed.), ASM Materials Science Seminar, ASM, Metals Park, OH (1981).

[20] D.A. Speck and B.R. Micciolo, **Advanced ceramic systems for rocket nozzle applications**, Carborundum Company Report (1968).

[21] A.T. Santhanam, P. Tierney and J.L. Hunt, **Metals Handbook: Properties and Selection**, Vol. 2, 10th edition, 950 (1990).

[22] D.J. Ham and J.S. Lee, **Transition metal carbides and nitrides as electrode materials for low temperature fuel cells**, Energies 2(4), 873 (2009).

[23] D.V. Esposito, S.T. Hunt, A.L. Stottlemyer, K.D. Dobson, B.E. McCandless, R.W. Birkmire and J.G. Chen, **Low-cost hydrogen evolution catalysts based on monolayer platinum on tungsten monocarbide (WC) substrates**, Angew. Chem. Int. Ed. 49, 9859 (2010).

[24] Y.C. Kimmel, L. Yang, T.G. Kelly, S.A. Rykov and J.G. Chen, **Theoretical prediction and experimental verification of low loading of platinum on titanium carbide as low-cost and stable electrocatalysts**, J. of Catal. 312, 216 (2014).

[25] W.F. Chen, J.T. Muckerman and E. Fujita, **Recent developments in transition metal carbides and nitrides as hydrogen evolution electrocatalysts**, Chem. Commun. 49, 8896 (2013).

[26] S. Wirth, F. Harnisch, M. Weinmann and U. Schröder, **Comparative study of IVb-VIb transition metal compound electrocatalysts for the hydrogen evolution reaction**, Appl. Catal. B 126, 225 (2012).

[27] D.D. Vasić, I.A. Pašti and S.V. Mentus, **DFT study of platinum and palladium overlayers on tungsten carbide: structure and electrocatalytic activity toward hydrogen oxidation/evolution reaction**, Int. J. Hydrogen Energy 38(12), 5009 (2013).

[28] E.C. Weigert, A.L. Stottlemyer, M.B. Zellner and J.G. Chen, **Tungsten monocarbide as potential replacement of platinum for methanol electro-oxidation**, J. Phys. Chem. C 111(40), 14617 (2007).

[29] I.J. Hsu, D.A. Hansgen, B.E. McCandless, B.G. Willis and J.G. Chen, **Atomic layer deposition of Pt on tungsten monocarbide (WC) for the oxygen reduction reaction**, J. Phys. Chem. C 115(9), 3709 (2011).

[30] S. Wirth, F. Harnisch, M. Weinmann and U. Schröder, **Comparative study of IVB-VIB transition metal compound electrocatalysts for the hydrogen evolution reaction**, Appl. Catal. B 126, 225 (2012).

[31] A. Joly, **Recherches sur les composes du nobium et du tantale**, Ann. Sci. Ecole Norm. Super (Paris) 6, 125 (1877).

[32] V.P. Elyutin, P.F. Merkulova, and Y.A. Pavlov, Proizv. i Obrabotka Stali i Splavov, Moskov, Inst. Stali im I. V. Stalina, Sb. 38, 79 (1958).

[33] G.P. Shveikin, Tr. Inst. Khim., Akad. Nauk SSSR, Ural'sk. Filial p. 51 (1958).

[34] F.G. Kusenko, and P.V. Gel'd, Izv. Vysshikh Uchebn. Zavendenii, Tsvetn. Met. 4, 43 (1961).

[35] M.L. Pochon, C.R. McKinsey, R.Á. Perkins, and W.D. Forgeng, Metallurgical Society Conference, Vol. 2 : "Reactive Metals" Wiley (Interscience), New York, 327, (1959).

[36] R.P. Elliott, ARF-2120-4 (Armour Research Foundation of the Illinois Institute of Technology, Technology Center, Chicago, Illinois), Trans. Am. Soc. Metals S3, 13 (1959).

[37] H. Kimura and Y. Sasaki, **The phase diagram of the niobium-carbon system**, Trans. Japan Inst. Metals 2, 98 (1961).

[38] J.F. Smith, O.N. Carlson, **The niobium-carbon system**, Journal of Nuclear Materials 148, 1 (1987).

[39] C.P. Kempter, A.K. Storms and R.J. Fries, **Lattice dimensions of NbCas a function of stoichiometry**, J. Chem. Phys. 33, 1873 (1960).

[40] Edmund K. Storms,**The refractory carbides**, Academi Press Inc. ltd., London (1967).

[41] E.J. Jr. Huber, E.L. Head, C.E. Jr. Holley, A.K. Storms and I.H. Krikorian, **The heats of combustion of niobium carbides**, J. Phys. Chem. 65, 1846 (1961).

[42] L.S. Levinson, **High-temperature heat content of niobium carbide and of tantalum carbide**, J. Chem. Phys. 39, 1550 (1963).

2. Literature Review:

A brief introduction of this different class of materials i.e. TMCs has been described in previous chapter. F.A. Cotton, G. Wilkinson and L.E. Toth, E.K. Storms had categorized TMCs as per their different characteristics. Among all TMCs, niobium carbide (NbC) attains an essential importance as an industrial material. To synthesize this particular compound is also a critical process because its desired properties depend on synthesis procedure which is in practice since early 20th century. Some of the latest developments are being considered as important one and are summarized here.

In 1986, **Gusev and Rempel** [1] is the group who adopted solid state diffusion to synthesize the niobium carbide in which they used solid state sintering of metallic niobium and carbon powder at a temperature of 2027 °C under 0.01 Pa vacuum for 20 hours. They observed homogeneous and single phase niobium carbide NbC_x which possess B1 or fm-3m (fcc space group) structure, where $0.97< x <0.72$. However, with the variation of annealing temperature, annealing time and cooling rate that the phase transition over which contains five non-equivalent superstructures of niobium carbide. After a decade in 1993, **Dal *et al.*** [2] intimated the carbothermal reduction of composite of polyacrylonitrile (PAN) with layered oxides of niobium ($(C_6H_{13}NH_3)Nb_3O_8$, $(C_8H_{17}NH_3)Nb_3O_8$) and tungsten ($(C_6H_{13}NH_3)NbWO_6$) at 1000 °C. They observed that the formation of cubic NbC is carried on via NbO_2 formation at 800 °C. The increase in the carbon content from 0.65 to 0.95 with the heating time at 1000 °C was observed. In the case of mixed carbide, cubic NbC and hex-WC got separated from each other in the reaction occurred at higher than 1000 °C.

In 1995, **Silva *et al.*** [3] suggested carbonaceous atmosphere to synthesize TMCs. In this method, they used a hydrocarbon gas as carbon source and hydrogen gas as a reducing agent with a fixed volume ratio. For their work, they took 0.001505 moles of B-Nb_2O_5 and CH_4/H_2 as precursors and heated this mixture to 1100 °C with different heating rate and molar space velocities and then

the reactor was quenched by removing from the furnace and allowed to cool to room temperature. They suggested that Nb_2O_5 reduced to lower oxides of niobium (NbO_2) and then NbO_2 is further reduced and carburized simultaneously. They concluded that there was not a significant effect of molar space velocities on the specific surface area of NbC nanoparticle and transition is pseudomorphic process which was supported by SEM micrograph. In the sequence to modify the synthesis route **Wong *et al.*** [4] synthesized TiC and NbC nano rods in early-1996. They took Ti and Nb iodide with CNTs at various -temperatures to observe the growth path of metal carbide nanotubes and nanorods. The reaction of Ti/Nb metal with CNTs in the presence of iodine gas was initiated by the formation of layer of TiC/NbC and followed by the inward growth of TiC/NbC until the nanorods were obtained. They concluded that the morphology of NbC and TiC nanorods are controlled by the CNTs which followed the template mechanism and nanotubes could be produced by controlling the growth parameters.

In this sequence, in 1997 **Tsuchida and Azuma** [5] suggested a different technique to synthesize NbC in which they took niobium (fixed amount) and carbon powder with different mole fractions (10-80%). They milled this mixture of Nb and C for different time intervals. When they exposed this activated mixture to air in graphite crucible, it resulted into a spontaneous exothermic reaction and self-propagating high temperature synthesis took place. Niobium mono-carbides (NbC) and semi-carbides (NbC_x) were obtained as major products and niobium nitride as minor product because the N_2 content in the atmosphere. The confirmation was carried out with the help of XRD analysis by which they concluded that the amount of mono carbide and semi carbide were increased with the increase in the content of activated carbon.

After a long synthesis practice of nano NbC, in 1999, **Xu *et al.*** [6] synthesized the NbC-3D network by using Nb_2O_5, sucrose ($C_{12}H_{22}O_{11}$) and NaCl as precursors. They mixed these precursors in agate mortar for 1 hour taking in ratio of 1:4:4 (respectively) and then heated the mixture in furnace upto 1120 °C with heating rate 15 °C/minute under 0.1 MPa/N_2 environment

and held for 0.5-2.0 hours. They confirmed the synthesis of cubic NbC by using XRD and SEM. This synthesis route was not as effective as gaseous atmosphere route was. In 1999, **Fukunaga *et al.*** [7] proposed a vapor solid reaction route for the synthesis of NbC. In this route they used carbon nano-tubes (CNTs), niobium powder and iodine which were packed in quartz ampoules of 5mm diameter. Due to very small size of CNTs, they possess very high reactivity at much lower temperature and tend to from the bond with niobium. The molar concentration ratio was 10:10:1 respectively. This mixture was heated upto different temperatures varying from 620 to 1000 °C for greater than 12 hours as holding period. They confirmed the structure by using XRD, TEM and HR-SEM. For the reactions at higher temperatures, coarsened NbC nanoparticle was observed with spherical or faceted morphology. They concluded that nanotube to nanoparticle transition occurred when synthesis temperature was increased. But the appearance of carbon in nano scale was the major drawback of this synthesis route. In the next year (2000), **J.B. Claridge *et al.*** [8] introduced the Temperature Programmed Reaction (TPR) synthesis of various transition metal carbides from their binary and ternary oxides using CH_4 and C_2H_6 as carbon source and appropriate catalyst. They prepared pallets of transition metal oxide precursors and heated the system in Pt crucible at different temperatures for different time periods. The confirmation was done by XRD, SAED and BET studies. They concluded that reaction required longer time when CH_4 was used as carbon source than that is required in the case of C_2H_6. The TPR route was quite similar to solid-gas reaction in carbonaceous environment route. It was very efficient to produce nanoparticles of NbC at a bulk scale.

In 2002, **Medeiros *et al.*** [9] used different precursors for the synthesis of NbC. It could change some output efficiency by changing input precursors. They varied the conventional precursors like oxides and modified its chemical state. They used niobium-oxalate complex compound (3 gms) as niobium source and H_2/CH_4 as reaction atmosphere. They carried this solid gas reaction at relatively low temperature i.e. 950 °C with slow heating rate (5 °C/min). In this synthesis

route, they fixed the flow rate of carbon source (CH_4) i.e. 20 lt/hour and hold the system for 2 hours at 950 °C. The final product of synthesis was characterized by XRD, TG/DTG and SEM analysis and concluded that the morphology of resultant NbC is similar to that of reactant. After the variation in raw materials for the synthesis of nano powder, in 2004 **Fontes *et al.*** [10] tried to change the reaction apparatus. To design a rotating cylinder for the synthesis of NbC powder by carbothermal reduction reaction was their idea to enhance the quality and quantity of synthesized NbC. In this process they used 0.004 kg of Nb_2O_5 with 20% (v/v) CH_4/H_2 as precursors. This mixture was heated to 900 °C at the heating rate of 10 °C/min. During all this process, the concentration of carbon source i.e. CH_4 was kept on decreasing as it was used for replacing the oxygen atom in Nb_2O_5. So, the total reaction time was decided on the basis of concentration of CH_4. The end synthesized nano powder (NbC) was confirmed by using XRD and SEM and then tried to optimize the operating parameters. Along with this **Liao *et al.*** [11] tried to deposit NbC thin film on NbC target by rf magnetron sputtering unit. In their practice, low oxygen impurity and maximum carbon content during the deposition was achieved, while the chemical etching or physical scattering was suggested as the cause of loss of carbon content in the film.

In all the above works, they were synthesizing nano NbC at elevated temperatures. All of them practiced with various operating conditions, but the synthesis temperature lower than 600 °C was attempted by **Shi *et al.*** [12] in 2005 and they were succeeded to embrace the co-reduction reaction route to synthesize the nano-crystalline NbC at low temperature 550°C. They chose anhydrous $NbCl_5$, CCl_4 and metallic Na in the molar ratio of 1:1:9 in glass lined stainless steel autoclave of 50 ml capacity and heated the sealed autoclave to 550 °C for 8 hours. The final gray powder of NbC was characterized by XRD, XPS, TG/DTG and TEM.

In 2008, **Miyajima *et al.*** [13] suggested changing the synthesis route completely. They adopted a supersonic source from a solenoid pulsed valve to synthesize NbC, in which they took a niobium metal rod and a graphite rod. They set down the stream of the supersonic source. The rods were

irradiated with tightly focused laser pulses (~10 mJ/pulse) at a wavelength of 532 nm and from a laser for generating the plasma. The evaporated niobium atoms and carbon atoms were cooled in the gas phase by the He gas under the pressure of 9 atm from the valve, forming Nb_nC_{m+} clusters. They observed the reactivity of this meta-stable compound with H_2 within the gas chamber. In 2009, **Giordano *et al.*** [14] produced several metal carbides at relatively low temperature (800 °C) using simple and mainly nontoxic precursor is presented. The procedure had been shown to be rather general and it was possible to synthesize NbC, TiC, WC, Mo_2C, and Cr_3C_2 nanoparticles using urea as carbon source and the growth controlling system. In every case, a homogeneous gel-like starting product had been formed that was converted by calcination into the metal carbide without any preliminary treatments or further purifications. Samples were characterized by XRD, TEM, SEM, elemental analysis, and BET. In this sequence **Choi** [15] practiced the conventional H_2/CH_4 environment route varying the heating rate and mass flow rate of gas. He used different amount of CH_4 to carburize fixed amount of Nb_2O_5 per unit time that is molar hourly space velocity (MHSV) with different heating rates and H_2/CH_4 ratio. They heated the mixture in quartz reactor to 800 °C in 90 minutes and rose to 1040 °C in 1 hour then allowed rapid cooling by removing it from the furnace. When reactor reached to room temperature the gas was changed to the He gas for 30 minutes and then 1% O_2/He for 2 hours passivation period. Then NbC sample was characterized by XRD and BET for ammonia conservation and oxygen uptake measurement. After Shi et al., the use of autoclave was repeated by **Ma *et al.*** [16] in 2009. He used magnesium and its compound ($MgCO_3$) for the synthesis and prepared nano-crystalline NbC at 550 °C. X-ray powder diffraction pattern indicated that the product was cubic niobium carbide. TEM confirmed that it consisted of particles with an average size of about 30 nm in diameter. The product was also studied by BET and TGA. It had good thermal stability and oxidation resistance below 400 °C in air. Recently in 2010, **Grove *et al.*** [17] proposed arc discharge apparatus to synthesize nano NbC. This synthesis route was very different from rest of

all suggested methods in recent years. They chose pure metal niobium rods (6.4 mm in diameter) as electrodes. Various concentrations of methane (2.5%, 50%, and 100%), ethylene (10%, 25%, 50%, 75%, and 100%), and acetylene (10%, 25%, 50%, 75%, and 100%) gases were seeded in the He gas and studied upon interactions with Nb. The gas mixture flow rate was maintained at 40 standard cm^3/min (SCCM) and a discharge was acquired by applying 180 amp direct current for a period of 10 min. The nanoparticles were collected using a bubbler containing acetonitrile. The samples were then sonicated for 15 min to ensure the nanoparticles were well suspended. TEM, EDS, and SAED were used to investigate the synthesized NbC nanoparticles, whereupon it was found that these nanoparticles adopt cubic morphology with methane gas, a mixture of cubes and cub-octahedron morphology with ethylene gas, and solely cube octahedron morphology with acetylene gas.

In mid-2011, **Zou *et al.*** [18] postulated that the anisotropy of CNTs can alter the superconducting characteristics of NbC when they are aligned to the magnetic field. They calculated the value of upper critical field is 4.2 T which is quite higher than reported earlier i.e. 1.7 T for pure bulk NbC. The CNT-NbC composites were formed through thermal reaction under controlled environment. CNT forests were soaked by the Nb precursor solution. The CNT forests containing Nb precursor solution were heated to 650 °C at a rate of 10 °C min^{-1} in the mixture gases of ethylene and forming gas. The sample was annealed at 650 °C for 1hour. The mixture gases were switched to Ar while the furnace was ramped to 1000°C in 1hour. The sample was annealed at this temperature in Ar for 3hrs. Finally, the sample was naturally cooled to room temperature by turning off the power supply to the furnace.

In 2013, **Woydt and Mohrbacher** [19] produced Niobium carbide from a commercially available high purity niobium pentaoxide (Nb_2O_5) powder. In this process lignite (coal) was blended with Nb_2O_5 powder and subsequently loaded into a furnace that was pre-heated to a temperature slightly above 1200°C under a mixture of 5% H_2-95% N_2 as operating atmosphere.

The progress of the carburization reaction was monitored by measuring the CO (g) concentration in the out-going gas. After completed carburization the sample material was moved into a cooling zone and held under a slightly reducing atmosphere consisting of N_2/H_2. They concluded that the tribological profile of NbC revealed a strong position under tribological considerations among other ceramic materials. In this queue **Qui *et al.*** [20] obtained NbC nanowire by bamboo based carbothermal route. In this synthesis process, Nb-Ni-F emulsion was prepared using Nb_2O_5, NaF, and $Ni(NO_3)\cdot 6H_2O$ which were dissolved in ethanol under ultrasound irradiation. Then dried bamboo chips were immersed in this emulsion followed by stirring and different thermal treatments at 80, 90 and 110 °C before heating it at 1250 °C in a sealed graphite crucible for 2 hours under the environment of argon. Then the furnace was allowed to cool to room temperature and argon flow was terminated below 150 °C. This synthesized nanowire was characterized by SEM, TEM, HR-TEM and electro-catalytic activity. As a result they suggested promising application as catalysts support in direct methanol fuel cells.

After so much of synthesis of nano particles, in 2014 **Zhang *et al.*** [21] proposed a direct current reactive magnetron sputtering to synthesize thin film of NbC using CH_4 as a carbon source on Si(100) as substrate. With increasing flow of CH_4 from 4 to 22 SCCM, the carbon content for the film was increased from 32.7 to 68.7 at.% gradually, accompanying with a phase transition from hexagonal-Nb_2C to cubic-NbC, and at the highest carbon content. The deposited NbC film exhibited a typical nano composite structure consisting of NbC nano-crystallites embedded in an amorphous hydrocarbon matrix. For the confirmation of the deposition of NbC thin film, they characterized the sample by XRD, XPS, SEM, HRTEM and AFM. While **Yate *et al.*** [22] tailored NbC thin film on the substrate of Si (100) and polystyrene at room temperature by non-reactive magnetron sputtering from pure Nb and C targets without applying bias voltage to the substrates. It was found that the films composed of 8-10% free-carbon exhibited a relatively high hardness, elastic recovery and electrical conductivity. This study indicates the potential of this

approach in depositing hard, elastic and electrically conductive nano composite films, which is especially useful for preparation of films on temperature sensitive polymers or plastic substrates for nano- and micro- electronics applications. In the same year **Zhang *et al.*** [23] intimated that doping of single atom niobium in graphitic structure may enhance electrochemical stability of catalytically active single atom sites by easing the penetration of oxygen into the graphite structure which is required in oxygen reduction reaction. For this purpose, modified arc discharge equipment with extra pure niobium rod (anode), carbon rod (cathode) and water cooled copper stage was used. The sample chamber was evacuated and at a certain pressure CH_4 was introduced as carbon source. The arc discharge enabled the evaporation of niobium from anode and carbon from the decomposition of methane which was combined to Nb to form NbC and simultaneously deposited on the cool chamber walls. For further confirmations, XRD, TGA, EELS, STEM and electrochemical test were carried out.

After so much practices of synthesis of nano NbC, in 2015 **Shiri *et al.*** [24] suggested to prepare Cu/NbC nano composite by high energy disc milling route. In this route they chose powders of copper, niobium and graphite and milled them for 7 hours in argon atmosphere. And then composite samples were made by two-step pressing and sintering at 900 °C for 1 hour under vacuum. Microstructure, hardness and wear behavior of the synthesized samples were observed to check the compatibility in the electrical contact application where electrical conductivity of copper and wear resistivity of NbC were optimized. The synthesized samples showed both the characters very well by the availability of Cu layer and NbC layer for respective uses. **Atchinson *et al.*** [25] proposed a route to prepare metal carbide/carbon composite fibers (ZrC/C, TiC/C and NbC/C). They prepared ZrC, TiC and NbC engulfed in the matrix of disordered carbon. The nano regime (high surface area of composite) and very high content of disordered, porous carbon make it as an ideal precursor to synthesize carbide derived carbon for electrochemical applications. They opted sol-gel technique in which cellulose acetate (carrier polymer) is mixed with titanium

butoxide, zirconium (IV) acetylacetonate, or niobium n-butoxide to obtain nano metal oxide/carbon composite and then carbothermal reduction transformed it into metal carbide/carbon at high temperature (1300-1700 °C). **Schmuecker and Leonard** [26] tried salt flux synthesis route for the formation of various TMCs (V_8C_7, TiC and TaC) to propose the reaction mechanism. For the preparation of the metal carbide, metal powder and multiwalled carbon nanotubes and added to a salt mixture consisting of lithium chloride, potassium chloride, and potassium fluoride. The reactants were placed in an alumina crucible and heated at 100°C/hour in a tube furnace to the desired temperatures under flowing argon. Most samples were quickly cooled (quenched) upon reaching the given interval temperature, to stop the reaction and trap the intermediates. The samples were quenched by removing the reaction tube from the heating coils and allowing them to quickly cool ~800 °C per hour to room temperature (25 °C) during which the freezing temperature of the eutectic salt is obtained quickly, below 353 °C.

It is very much clear that various kinds of synthesis routes have been adopted by numerous people to get optimized form of NbC. Amongst all of the reported routes, the most convenient process is solvothermal route adopted by Ma *et al.* [16] and Shi *et al.* [12] because of its simplicity, easy maintenance, design, manufacturing cost, maintenance with cheaper ingredients and higher purity of synthesized sample. Ma *et al.* [12] practiced almost all the carbides (NbC, TaC, VC, TiC) using autoclave but the impurity phase such as lower oxides or semi-carbides were present in their samples of NbC [16, 27-29]. **Kumar *et al.* (2009, 2011)** fabricated tungsten carbide (WC) nano particle from different W-ores in which methanol, ethanol and acetone (carbon source) and magnesium metal powder (reducing agent) were kept in autoclave and heated to 600, 850 °C for a very long duration (15, 20 hours) [30, 31]. In this practice, they suggested the reaction kinetics and proposed the reaction mechanism involved in the chemical reaction for the formation of WC nano particle. After this **Singla *et al.* [32, 33]** modified the

reaction parameters by changing the synthesis duration (lower time duration) and varying the amount of carbon source. They suggested the reduction path of WO_3 to W-metal followed by the carburization which results to the formation of WC nano particle. Using same route **Mahajan *et al.*** [34] and **Brar *et al.*** [35] optimized the reaction variables to produce vanadium carbide (VC) from vanadium pent-oxide, tantalum carbide (TaC) from tantalum ethoxide respectively and suggested the application of VC in the field of optical sensors with the help of photo-luminescence test and possibility of electrochemical applications of TaC which is governed by the carbon deficiency in the synthesized crystal [34, 35].

Basically, due to less stability over solid reactants and lower handling arrangements than gaseous reactants, liquid reactants are preferred for this process. Along with this, the vapor pressure of solvent plays very important role in the procedure at elevated temperatures. This autoclave can be designed at any scale considering the various processing parameters like temperature, capacity of production, pressure inside the autoclave and amount of reactants etc. Pressure and temperature are the most critical parameters for the designing of autoclave. Mass production of TMCs is possible via this route. As compared to other routes, this route is quite cheap because there is no need of any special instrument such as rotating cylinder for synthesis, or no need of special sophisticated technique like arc discharge apparatus and any special precursors for the transformation to carbide.

Therefore, the effect of processing temperature and time duration needs to be optimized to obtain single phase NbC and the effect of these parameters on the crystal properties and reaction kinetics i.e. diffusion of carbon and reduction of raw material (niobium pent-oxide) should be observed. The experimental procedure will elaborate the synthesis process along with the characterizations involved for the various structural and thermal confirmations.

2.1. References:

[1] A.I. Gusev and A.A. Rampel**, Order-disorder phase transition channel in niobium carbide,** Phys. Stat. Sol. (A) 93, 71 (1986).

[2] B.F. Dal, S.G. Hardin, D.G. Hay and T.W. Turney, **Selective, low temperature synthesis of niobium carbide and mixed (niobium/tungsten) carbide from metal oxide-polyacrylonitrile composites by carbothermal reduction,** J. Mat. Sci. 28, 6657 (1993).

[3] V.L.S. Teixeira da Silva, E.I. Ko, M. Schmal, and S.T. Oyama, **Synthesis of niobium carbide from niobium oxide aerogels,** Chem. Mater. 7, 179 (1995).

[4] E.W. Wong, B.W. Maynor, L.D. Burns and C.M. Lieber, **Growth of metal carbide nanotubes and nanorods,** Chem. Mater. 8, 2041 (1996).

[5] T. Tsuchida and Y. Azuma, **Synthesis of niobium carbide and nitride in air from mechanically activated Nb-C powder mixtures,** J. Mater. Chem.7 (11), 2265 (1997).

[6] G.Y. Xu, Y. Huang, J.B. Li and Z.P. Xie**, Low-temperature synthesis of niobium carbde three-dimensional netted fibres by the carbothermal method,** J. of Mat. Sci. Lett. 18, 827 (1999).

[7] A. Fukunaga, S. Chu, M.E. Henry and M. Nagumo, **Synthesis, structure and superconducting properties of NbC nanorods and nanoparticles,** Mat. Trans., JIM 40(2), 118 (1999).

[8] J.B. Claridge, A.P.E. York, A.J. Brungs and M.L.H. Green, **Study of temperature programmed reaction synthesis of early transition metal carbide and nitride catalyst materials from oxide precursors,** Chem. Mater. 12, 132 (2000).

[9] F.F.P. Medeiros, A.G.P. da Silva, C.P. de Souza, **Synthesis of niobium carbide at low temperature and its use in hardmetal,** Powder Technology 126, 155 (2002).

[10] F.A.O. Fontes, K.K.P. Gomes, S.A. Oliveira, C.P. Souza and J.F. Sousa, **Niobium carbide synthesis by solid gas reaction using a rotating cylinder reactor,** Braz. J. of Chem. Eng. 21(3), 393 (2004).

[11] M.Y. Liao, Y. Gotoh, H. Tsuji and J. Ishikawa, **Compound-target sputtering for niobium carbide thin film deposition,** J. Vac. Sci. Tech B 22(5), L24 (2004).

[12] L. Shi, Y. Gu, L. Chen, Z. Yang, J. Ma and Y. Qian, **Synthesis and oxidation behavior of nanocrystalline niobium carbide**, Solid State Ionics 176, 84 (2005).

[13] K. Miyajima, N. Fukushima, and F. Mafune, **Reactivity of niobium-carbon cluster ions with hydrogen molecules in relation to formation mechanism of met-car cluster ions**, J. of Phys. Chem. (A) Lett. 112, 5774 (2008).

[14] C. Giordano, C. Erpen, W. Yao, B. Milke, and M. Antonietti, **Metal nitride and metal carbide nanoparticles by a soft urea pathway**, Chem. Mater. 21, 5136 (2009).

[15] J.G. Choi, **Preparation and characterization of niobium carbide crystallites,** J. of Korean Cryst. Growth and Cryst. Tech. 19(3), 125 (2009).

[16] J. Ma, M. Wu, Y. Du, S. Chen, W. Jin, L. Fu, Q. Yang and A. Wen, **Formation of nanocrystalline niobium carbide (NbC) with a convenient route at low temperature,** J. of All. &Comp. 475, 415 (2009).

[17] D.E. Grove, U. Gupta and A.W. Castleman Jr., **Effect of hydrocarbons on the morphology of synthesized niobium carbide nanoparticles**, Langmuir 26(21), 16517 (2010).

[18] G.F. Zou, H.M. Luo, S. Baily, Y.Y. Zhang, N.F. Haberkorn, J. Xiong, E. Bauer, T.M. McCleskey, A.K. Burrell, L. Civale, Y.T. Zhu, J.L. MacManus-Driscoll and Q.X. Jia,

Highly aligned carbon nanotube forests coated by superconducting NbC, Nature Communications, DOI: 10.1038/ncomms1438 (2011).

[19] M. Woydt, H. Mohrbacher**, Friction and wear of binder-less niobium carbide,** Wear 306, 126 (2013).

[20] Z. Qiu, H. Huang, J. Du, T. Feng, W. Zhang, Y. Gan, and X. Tao, **NbC nanowire-supported Pt nanoparticles as a high performance catalyst for methanol electro-oxidation**, J. Phys. Chem. C 117, 13770 (2013).

[21] K. Zhang, M. Wen, G. Cheng, X. Li, Q.N. Meng, J.S. L and W.T. Zheng, **Reactive magnetron sputtering deposition and characterization of niobium carbide film,** Vacuum 99, 233 (2014).

[22] L. Yate, L.E. Coy, G. Wang, M. Beltr´an, E. D´ıaz-Barriga, E.M. Saucedo, M.A. Ceniceros, K. Załęski, I. Llarena, M. MÖller and R.F. Ziolo, **Tailoring mechanical properties and electrical conductivity of flexible niobium carbide nanocomposite thin films,** RSC Adv. 4, 61355 (2014).

[23] X. Zhang, J. Guo, P. Guan, C. Liu, H. Huang, F. Xue, X. Dong, S.J. Pennycook & M.F. Chisholm, **Catalytically active single-atom niobium in graphitic layers**, Nature Communications, DOI: 10.1038/ncomms2929 (2013).

[24] S.G. Shiri, P. Abachi, K. Pourazarang and M.M. Rahvard, **Preparation of in-situ Cu/NbC nanocomposite and its functionally graded behaviour for electrical contact applications**, Trans. Nonferrous Met. Soc. China 25, 863 (2015).

[25] J. Atchison, M. Zeiger, A. Tolosa, L.M. Funke, N. Jäckel and V. Presser, **Electrospinning of ultrafine metal oxide/carbon and metal carbide/carbon nano-composite fibers**, RSC Adv., DOI: 10.1039/C5RA05409E (2015).

[26] S.M. Schmuecker and B.M. Leonard, **Formation mechanism of nanostructured metal carbides via salt- flux synthesis,** Inorg. Chem, DOI: 10.1021/acs.inorgchem.5b00059 (2015).

[27] J. Ma, Y. Du, M. Wu and M. Pan**, One simple synthesis route to nanocrystalline tantalum carbide via the reaction of tantalum pentachloride and sodium carbonate with metallic magnesium**, Materials Letters 61(17), 3658 (2007).

[28] J. Ma, M. Wu, Y. Du, S. Chen, G. Li and J. Hu, **Synthesis of nanocrystalline titanium carbide with a new convenient route at low temperature and its thermal stability,** Mat. Sci.and Eng. B 153, 96 (2008).

[29] J. Ma, M. Wu, Y. Du, S. Chen, J. Ye and L. Jin**, Low temperature synthesis of vanadium carbide (VC)**, Materials Letters 63(11), 905 (2009).

[30] A. Kumar, K. Singh, O.P. Pandey, **Reduction of WO_3 to nano-wc by thermo-chemical reaction route** Physica E 41, 677 (2009).

[31] A. Kumar, K. Singh, O.P. Pandey, **Direct conversion of wolframite ore to tungsten carbide nano particles**, Int. J. Refract. Met. Hard Mater, doi:10.1016/j.ijrmhm.2011.01.009 (2011).

[32] G. Singla, K. Singh and O.P. Pandey, **Structural and thermal properties of in-situ reduced WO_3 to W powder,** Powder Technology 237, 9 (2013).

[33] G. Singla, K. Singh and O.P. Pandey, **Structural and thermal analysis of in situ synthesized C-WC nano composites,** Ceramics International 40, 5157 (2014).

[34] M. Mahajan, N.P. Lalla, K. Singh and O.P. Pandey, **Synthesis and photoluminescence properties of in-situ synthesized core shell (m-VC@C) nano-composites,** Mat. Chem. and Phy., doi:10.1016/j.matchemphys.2015.04.004 (2015).

[35] L.K. Brar, G. Singla and O.P. Pandey, **Evolution of structural and thermal properties of carbon coated TaC nanopowder synthesized by single step reduction of Ta-ethoxide,** RSC Advances, DOI: 10.1039/c4ra12105h (2014).

3. Experimental work:

In the present work, transition metal (Niobium) carbide i.e. NbC is synthesized at nano scale via carbothermal route using niobium pentaoxide (Nb_2O_5) as niobium source, acetone and activated charcoal as carbon source and magnesium (Mg) metal powder as reducing agent.

3.1. Material used: Niobium pentaoxide (Nb_2O_5, *Sigma-Aldrich, 99.99%*) was used as niobium source and for the addition of carbon to the niobium crystal, acetone (C_3H_6O, SDFC Ltd.) and charcoal (SDFC Ltd.) was used. Since charcoal is the direct source of carbon, there is no other reaction involved to extract carbon from its source. Acetone is a cheaper liquid source of carbon and charcoal is the cheapest solid state carbon source which made them to be used to synthesize. Further, to reduce the oxide precursor Magnesium metal powder (*Lobachemie, 99%*) is used.

3.2. Methodology: The detailed methodology followed is shown in figure 4. Though the experiments were performed at different temperatures for different duration but considering the aim to synthesize the carbide at low temperature, the condition used for 600 °C is given in table 3. However, the other conditions are discussed in the text.

Table 3: Details of synthesis conditions.

Sample Id	Carbon Source (Amount)	Synthesis Temperature (°C)	Impregnation Time (hrs)	Heating Rate (°C/min)
1N600 2.5	Acetone (10 ml)	600	1	2.5
1N600	Acetone (10 ml)	600	1	5
1N600 7.5	Acetone (10 ml)	600	1	7.5
2N600	Acetone (10 ml)	600	2	5
5N600	Acetone (10 ml)	600	5	5
7N600	Acetone (10 ml)	600	7	5
10N600	Acetone (10 ml)	600	10	5

5N700	Acetone (10 ml)	700	5	5
10N700	Acetone (10 ml)	700	10	5
5N800	Acetone (10 ml)	800	5	5
10N800	Acetone (10 ml)	800	10	5
10C600	Charcoal (1.5 gms)	600	10	5
10C700	Charcoal (1.5 gms)	700	10	5
10C800	Charcoal (1.5gms)	800	10	5

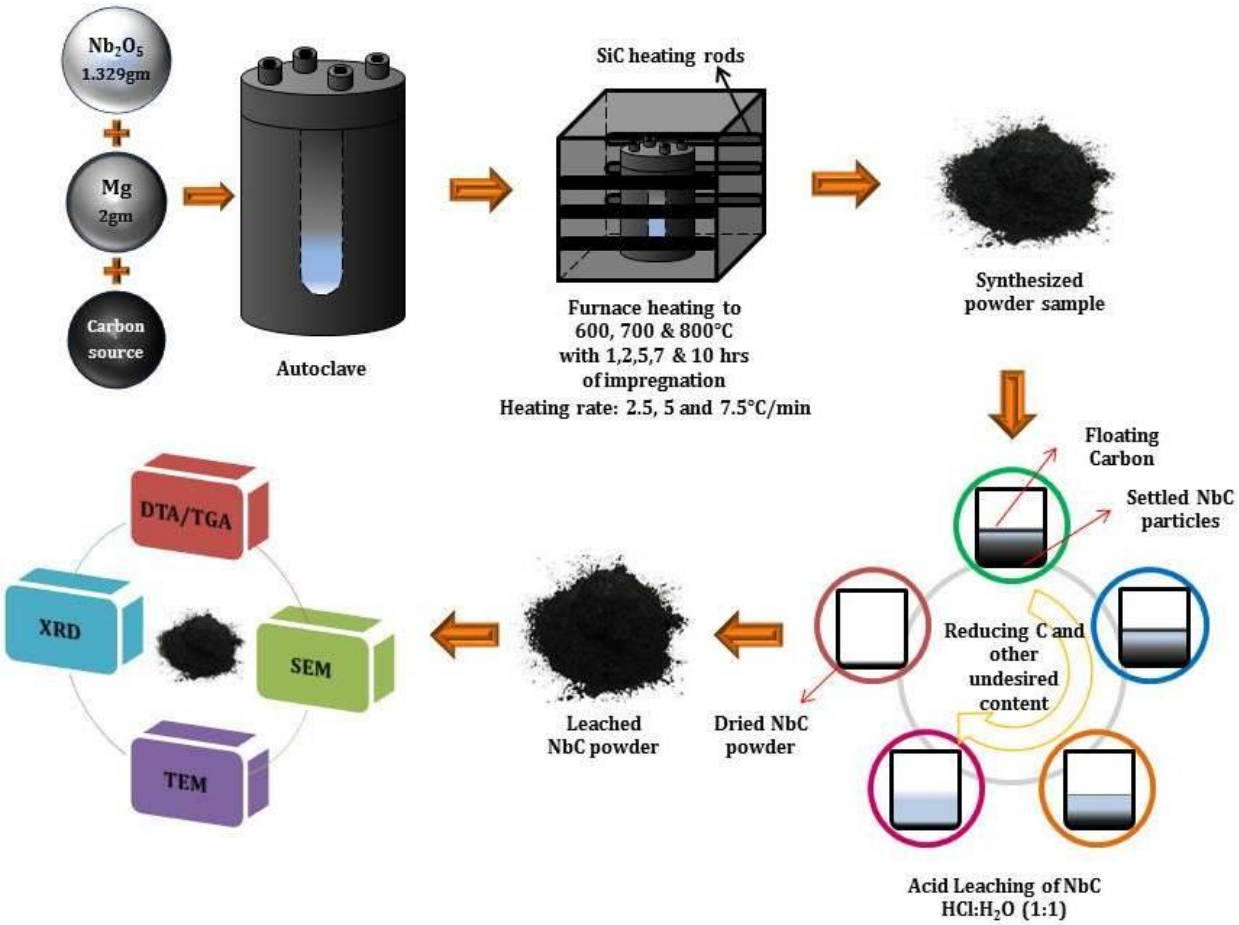

Figure 4: Methodology used to synthesize and characterize the nano niobium carbide (NbC).

3.3. Characterizations:

3.3.1. X-ray diffraction: XRD technique is a family of non-destructive analytical techniques which reveals the information about the crystallographic structure, chemical composition and physical properties of materials. X-rays possess the wavelength of the order of few angstroms,

which is comparable to the typical interatomic distance in a crystalline solid. Therefore, X-rays can be diffracted from atoms situated at their respective lattice sites. When certain geometric requirements are met, X-rays scattering from atoms interfere constructively, producing a diffracted beam. In 1912, W. L. Bragg recognized a predictable relationship among several factors. These factors are combined in Bragg's law as described below;

$$2d.\sin\theta = n\lambda$$

where 'd' is inter-planar distance and 'λ' is wavelength of incident X-ray, 'θ' is diffraction angle and 'n' is the order of the diffraction i.e. equal to 1 (for the most of the cases). The results will help to confirm that the obtained powder is crystalline, mono crystalline or amorphous. The extent of deviation from standard peak positions will help to calculate the strain present in the synthesized sample.

3.3.2. Differential Thermal Analysis (DTA)/Thermal Gravimetric Analysis (TGA):

DTA/TGA helps to analyze the liberation (exothermic reaction) and absorption (endothermic reaction) of heat, which is associated with physical and chemical changes that occurred in materials with the rise or fall in the temperature. Such information is essential for understanding thermal properties of materials. With the variation in temperature of the system (sample chamber), material starts changing its physical state via releasing or absorbing heat which results to the oxidation or reduction of material. This oxidation or reduction leads to gain or loss of weight of sample which is measured with the help of cantilever beam with respect to the reference material which is stable at operation range of temperature. This technique to measure the weight gain or loss of sample with respect to temperature change is referred as TGA. Both of these techniques give a detailed idea about the thermodynamics and kinetics of reactions involved in synthesis.

3.3.3. Scanning Electron Microscopy (SEM): SEM is an important tool for microstructural analysis. It provides the information regarding topographical features, surface morphology, phase

distribution, compositional differences, orientation order within the crystal and presence of defects with locations. The strength of SEM lies in its inherent versatility due to multiple signal generated, simple image formation process, wide magnification range and excellent depth of field. The SEM micrographs could be taken in two modes i.e. secondary emission mode and back scattered mode.

3.3.4. Transmission Electron Microscopy (TEM): Transmission electron microscopy (TEM) is a microscopy technique in which a beam of electron is transmitted through an ultra thin specimen. It interacts with the specimen as it passes through. An image is formed from the interaction of the electrons transmitted through the specimen; the image is magnified and focused onto the imaging device, such as fluorescent screen, on a layer of photographic film, or to be detected by a sensor such as CCD camera. At smaller magnifications TEM image contrast is due to absorption of electrons in the materials, due to thickness and composition of the materials. At higher magnifications complex wave interactions modulate the intensity of the image, requiring expert analysis of observed images. For TEM study the synthesized powder was suspended in ethanol. One drop of the suspension was dropped on carbon coated copper grid and alcohol was allowed to evaporate.

4. Results and Discussion:

In the proposed work, the synthesis of NbC is done to enhance the efficiency of procedure by decreasing the operating temperature and the continuance involved in it. Therefore, temperatures 600, 700 and 800 ºC were chosen to recite the synthesis. This variation of temperature leads to variation in crystal-structural, thermal and microstructural features of nano powder which are discussed in this chapter.

4.1. X-ray diffraction analysis:

The results of X-ray diffraction analysis were compared and matched with different standard ICDD cards in *PANalytical X'Pert Highscore* Plus tool to identify the constituted phases at various synthesis conditions. Almost all the obtained patterns contain 5 peaks of NbC which correspond to (111), (220), (200), (311) and (222) respectively. These peaks confirm the rock-salt (NaCl) structure of NbC having space group fm-3m. The standard cards from which peaks are being matched are enlisted below:

Table 4: List of ICDD cards used for phase determination.

S. No.	ICDD card	Phase	Crystal Structure
1	01-089-3690	NbC	FCC
2	00-019-0870	Nb_2C	Orthorhombic
3	01-082-1141 00-019-0859 01-074-1378	NbO_2	Tetragonal
4	00-019-0862 00-037-1468 01-071-0005	Nb_2O_5	Monoclinic
5	01-084-0455	$NbO_{0.76}$	FCC
6	00-042-1125	NbO	FCC
7	01-089-8487	C	Amorphous

In order to determine the information from the XRD peaks, all the patterns, peak positions and full width at half maxima (FWHM, βhkl) were measured by Gaussian fitting of peak profile which assumed the symmetric nature of peak profile. Lattice constant was calculated using Bragg's law, $\boldsymbol{d_{hkl} = \frac{n\lambda}{2\sin\theta_{hkl}}}$ and $\boldsymbol{a = d\sqrt{h^2 + k^2 + l^2}}$, which is nearly equal to standard value (4.4704 Å) as tabulated in table 5. Moreover, the variation from the standard values of lattice constants leads to the variation in carbon content in the crystal lattice of stoichiometric NbC which is also listed in table 5. Shi *et al.* [1] suggested that the dependency of carbon content (x) in non-stoichiometric niobium carbide (NbC_x) can be calculated by:

$$\boldsymbol{a(\text{Å}) = 4.09847 + 0.71820x - 0.34570x^2} \quad \textbf{(i)}$$

Table 5: Lattice constant and carbon content of synthesized samples.

Sample Id	Lattice constant (Å)	C- content (x)	Sample ID	Lattice constant (Å)	C-content (x)
1N600 2.5	4.4651	0.9037	10N600	4.4696	0.9644
1N600	4.4645	0.8971	5N700	4.4703	0.9792
1N600 7.5	4.4654	0.9061	5N800	4.4697	0.9665
2N600	4.4707	0.9919	10C700	4.4599	0.8563
5N600	4.4704	0.9831	10C800	4.4674	0.9306
7N600	4.4650	0.9021			

4.1.1. Effect of temperature on the synthesis of NbC:

Figure 5 shows the XRD pattern of synthesized powders at different synthesis temperatures (600, 700 and 800°C) and impregnation durations (5 and 10 hrs). It is clear from the XRD pattern that the synthesis of NbC at nano scale is fully governed by the synthesis conditions (the temperature as well as time). In starting, during impregnation at 800 °C for 10 hr, NbC was obtained along with oxide (NbO_2, Nb_2O_5, $NbO_{0.76}$). As the temperature is reduced to 700 °C, the decrease in the oxide content was observed (figure 1) which may be attributed to the carburization of niobium oxide at 700 °C due to the lack of thermal energy to oxidize NbC at lower temperature [2].

Further reduction in temperature to 600 °C leads to almost complete carburization of oxides. The effect of impregnation time at same synthesis temperature seems to promote the growth of carbide particles (intense peaks) which is shown in figure 5 for heating upto 5 and 10 hr at 700 and 800 °C. This process occurs because longer time promotes feasible diffusion of carbon into the lattice [3]. While at 600 °C with impregnation of 5 hours powder sample (5N600) contains single phase NbC along with the small carbon content. The effect of longer impregnation at 600°C leads to the formation of Nb_2O_5 which may be attributed to the oxidation of NbC. As shown in figure 5, a metastable phase $NbO_{0.76}$ is also obtained at 700 °C and 800 °C which is an intermediate stage of transformation of NbC_xO_y to NbO and promoted with longer impregnation [4]. Hence, the reaction kinetics of oxidation and carburization at different temperatures result to the transportation of oxygen and carbon atoms in the unit cell of niobium which imparts the enlargement or compression of crystallite. It can be observed from the figure 5 that beyond 600 °C, the mechanism of the formation of NbC has reversed by forming niobium oxides (Nb_2O_5, NbO_2) and 600 °C is the optimized temperature in this study.

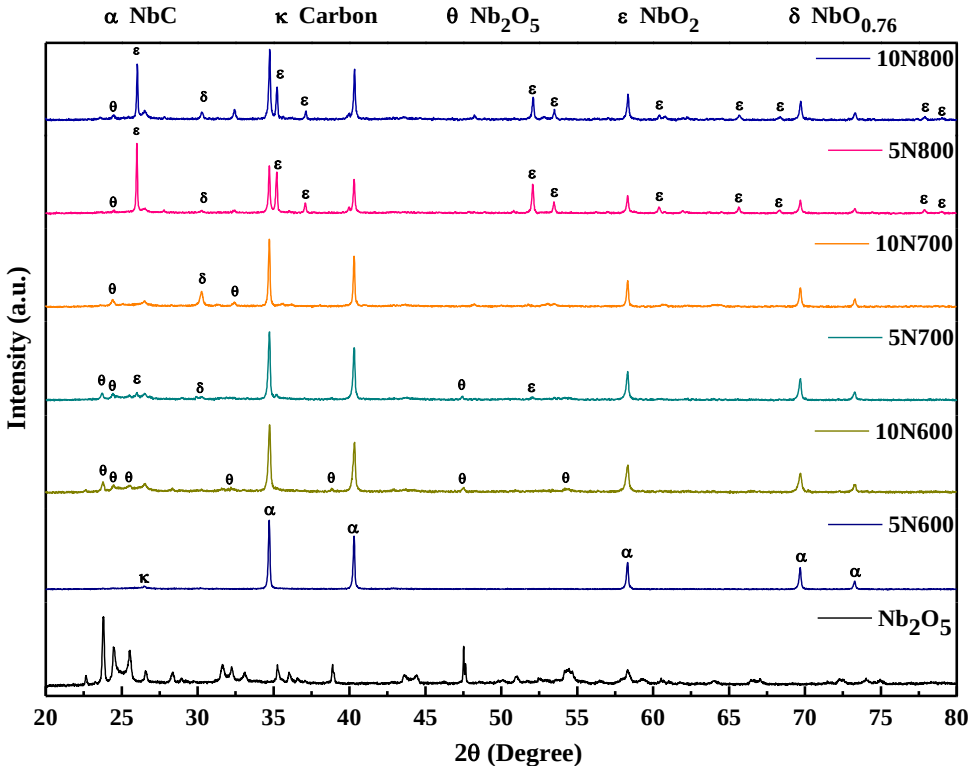

Figure 5: Effect of synthesis temperature on the developed phases during the formation of NbC.

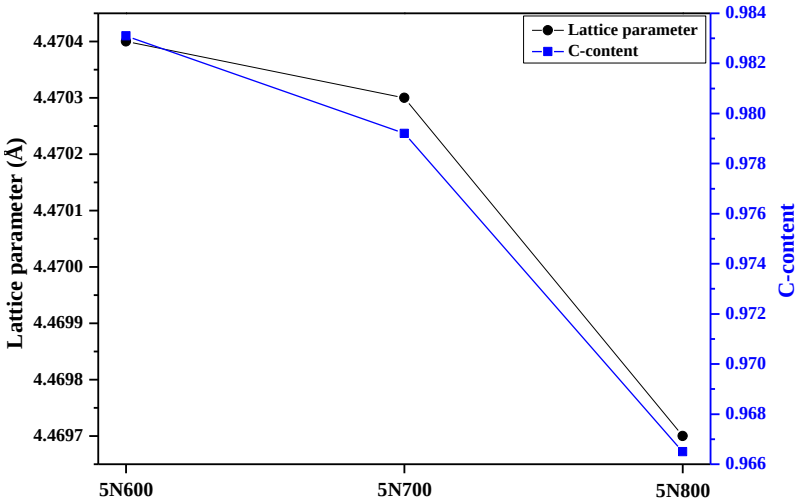

Figure 6: Variation of lattice parameter and carbon content at different synthesis temperature (600, 700 & 800 ºC).

The effect of synthesis temperature on the carbon content in synthesized sample calculated using equation (i) is shown in figure 6. The pattern as shown in figure 6 suggest that the decrement in lattice constant and carbon content is caused by the increased temperature which may be attributed to the oxidation of NbC. This variation in the carbon content with the temperature supports the broadening of peaks as shown in the XRD pattern (figure 5) which is associated with the simultaneous removal of carbon and absorption of oxygen causing distortion within the unit cell.

4.1.2. Effect of impregnation duration at 600 ºC on the composition of synthesized NbC powder:

As discussed in the earlier section after optimizing the synthesis conditions pure NbC nano powder has been obtained after heating for 5 hr at 600 °C. So in order to investigate the effect of impregnation time, autoclave has been heated for different time durations (1h, 2h 7h and 10h) at 600 °C. The effect of different impregnation time is clearly visible in figure 7 through XRD pattern. The presence of peak which corresponds to NbO_2 in sample 1N600 clearly designates the reduction of Nb_2O_5. However, with the further increase in the impregnation time, pure NbC nano powder has been obtained which remains stable upto 5 hr heating time. But with the further increase in the time a small peak of Nb_2O_5 in 7 hr indicates its reversibility with decarburization.

The formation of Nb_2O_5 may be caused due to the lower heat of formation of Nb_2O_5 (ΔG = -454.5 kcal.mole^{-1}) than NbO_2 (ΔG = -190.4 kcal.mole^{-1}) which may cause the formation of niobium penta-oxide [5]. Such kind of decarburization is also reported by Kim *et al.* [6] in their report. The detail reaction path is shown below:

$$NbC + O_2 \longrightarrow NbO_2 + C$$

$$4NbO_2 + O_2 \longrightarrow 2Nb_2O_5$$

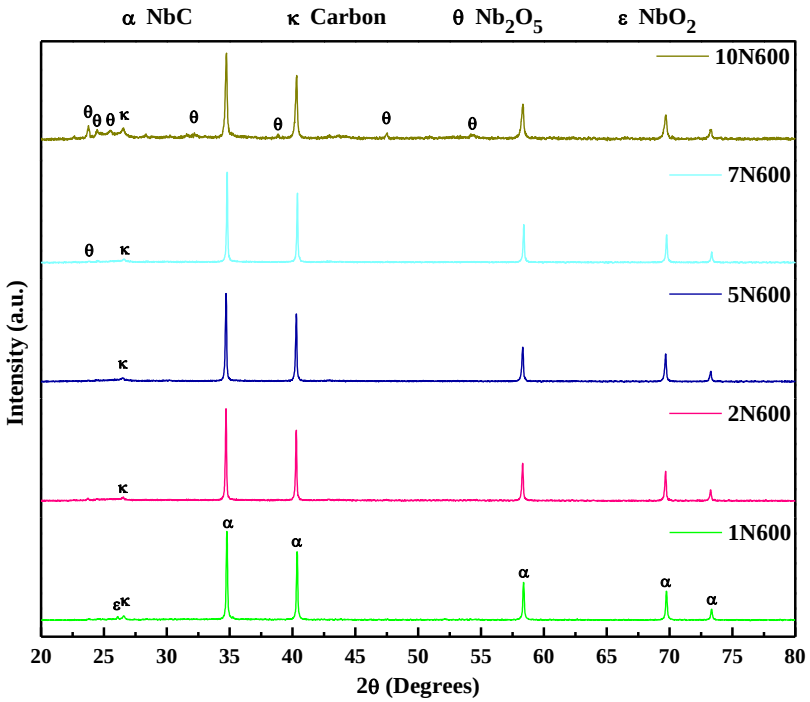

Figure 7: Effect of different impregnation periods at 600 °C on the synthesis of NbC.

Moreover, the effect of impregnation time on the correlations between carbon content and lattice constant is shown in figure 8. The same variations in lattice constant and carbon content with the time indicates that the lattice constant is fully depended upon the content of carbon in the lattice. Hence, figure 8 suggests a trend of decrement of carbon content and lattice parameter with increasing impregnation. But '7N600' shows a peculiar behavior which is out of the league. Between 5 and 7 hour impregnation, there is a critical value of time which initiates the oxidation and sudden carbon loss is observed at this configuration. Beyond 7hr impregnation (10hrs), the carbon content has been increased by forming higher amount of Nb_2O_5 at 600 °C which tries to

balance the niobium and carbon content in the unit cell of niobium and leads to the carbon content to 0.9644.

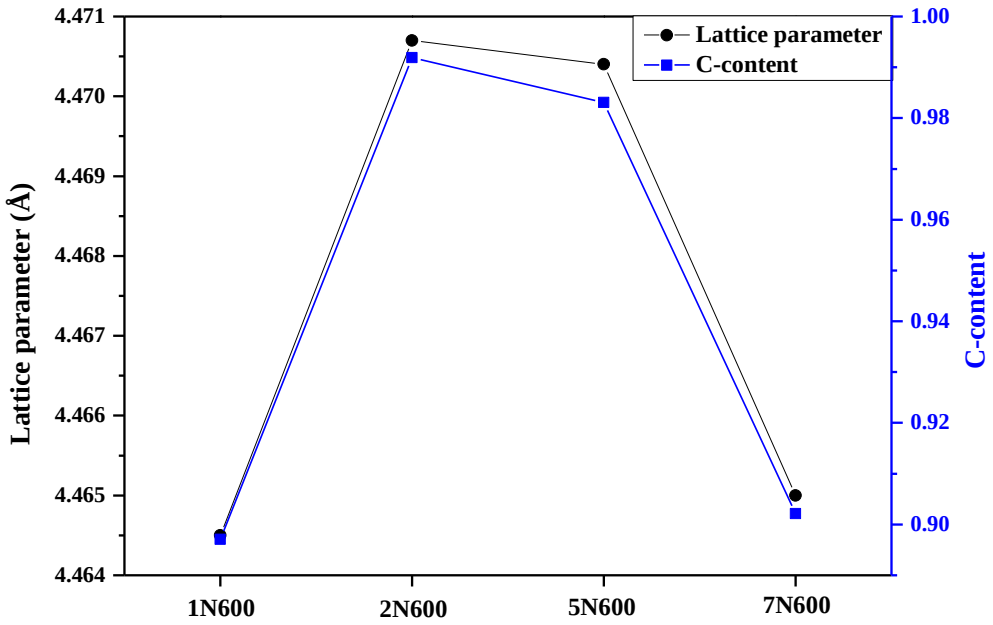

Figure 8: Variation of lattice parameter and carbon content at different impregnation time (1, 2, 5 and 7 hours) at 600 ºC.

4.1.3. Effect of heating rate on the NbC formation at 600 ºC with impregnation of 1 hour:

In other addition, the variability of heating rate also affects the NbC formation which is shown in figure 9 in which three heating rates (2.5, 5 and 7.5 °C/min) were practiced to understand this effect. From figure 9, it is very much clear that NbC can be obtained by heating the reactant mixture at all three heating rates. However, the sample heated at higher heating rate show lesser formation of NbC from Nb_2O_5 as compared to lower heating rate (2.5 °C/min). It means lesser heating rates provide sufficient time for the reduction as well carburization of oxide (s) which is clearly seen from the XRD pattern (figure 9) with the presence of higher content of NbC along with the lower oxide content as compared to '1N600' configuration. But, both the heating rates (2.5 and 5 °C/min) are not sufficient enough to transform whole Nb_2O_5 into NbC and result to the mixture of lower oxide (NbO_2) and NbC. In the case of 7.5 °C/min, homogenization of energy in the system is not obtained for the transformation of Nb_2O_5 to form NbC which is observed in the case of '1N600' and '1N600 2.5'. Hence, the heating rates control the reduction of Nb_2O_5 to form

NbO_2 and that's why lower rate (2.5 °C/min) leads to reduction in NbO_2 content in synthesized sample.

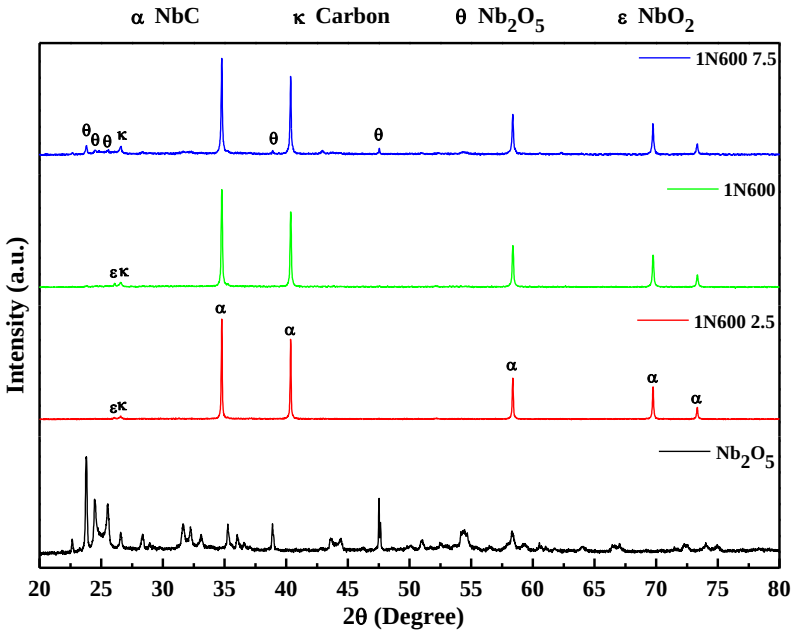

Figure 9: Effect of heating rate on the synthesis of NbC at 600 °C.

4.1.4. Effect of Carbon source to synthesize nano crystalline NbC:

After practicing the synthesis of NbC at various temperatures, impregnation and heating rates with liquid carbon source (acetone), charcoal was used as carbon source to carburize Nb_2O_5 instead of acetone to synthesize NbC at nano scale (figure 10). Figure 10 depicts that single phase NbC is obtained at 800 °C in 10h impregnation duration, while reduction in synthesis temperature to 700 °C leads to increase in non-stoichiometry and forms Nb_2C as minor phase as shown in figure 10 (marked with β). Further decrement in temperature suggested the formation of NbO (cubic) and very small amount of NbO_2 at 600 °C. The above discussion suggests a path of reduction and carburization of Nb_2O_5 to synthesize NbC via the formation of lower oxides (NbO_2, NbO) and semi carbides (Nb_2C) among all three temperatures, the highest temperature i.e. 800°C shows the single phase NbC XRD pattern with 0.93 carbon content.

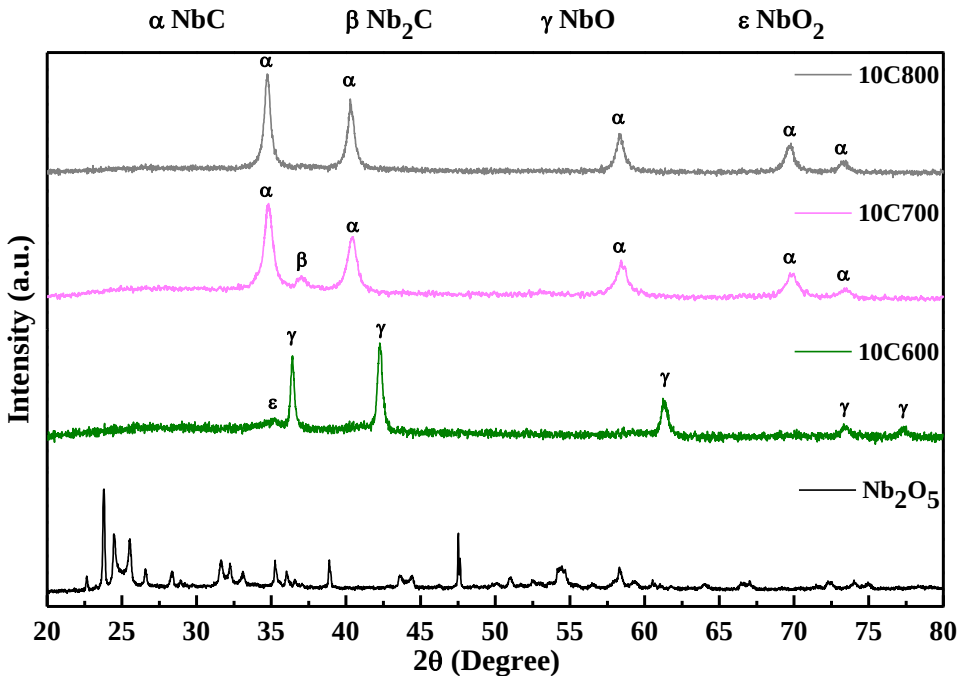

Figure 10: Effect of temperature on the synthesis of NbC using activated charcoal.

Comparing the figure 7 and 10, it can be postulated that the nature of peaks of NbC is quite broader when charcoal is used to synthesize NbC as compared to the case in which acetone is used. The broadness of peaks in sample '10C800' may be attributed due to the smaller size of crystallite and the higher amount of strain present in the crystallite of NbC which is calculated and discussed by Williamson-Hall analysis as discussed later. Single phase NbC pattern is obtained at different operating conditions in both of the samples '2N600' and '10C800'. In the case of '2N600', solid-liquid reaction occur in which fragmentation of Nb_2O_5 particle by hydrogen take place which further reduced by Mg and hydrocarbon [4, 7] make the chemical process feasible at lower temperature 600 °C. On the other hand, the absence of hydrogen in case solid-solid reaction and reduction of Nb_2O_5 by Mg and nascent carbon forming $MgO/CO/CO_2$ result to obtain single phase NbC pattern at 800 °C in '10C800'. The amorphous nature of carbon present in the powder sample can be confirmed by TEM analysis which will be discussed later in this chapter.

4.2. Williamson-Hall analysis:

X-ray line profile analysis depicts the logical extraction of size and distortion of the samples. Scherrer method is a versatile criterion for the determination of crystallite size for the coherent scattering in the sample. The crystallite size obtained from the Scherrer formula is volume weighted quantity which is associated with the full width at half maxima (β_{hkl}) and is given as

$$\boldsymbol{t = \frac{k\lambda}{\beta_{hkl}\cos\theta_{hkl}}} \quad \textbf{(ii)}$$

where k: shape factor (~1), θ: Bragg angle and λ: X-ray wavelength (~0.15406 nm). The peak broadening is solely attributed to the crystallite size, while Stokes and Wilson proposed the mathematical formulation of peak broadening due to strain [8]. The induced strain (ε) in the crystal can be expressed as

$$\boldsymbol{\beta = 4.\varepsilon.tan\theta_{hkl}} \quad \textbf{(iii)}$$

Thus, the observed FWHM is the combination of equation (i) and (ii) and Williamson-Hall plot is used to separate the individual effects:

$$\boldsymbol{\beta_{hkl}\cos\theta_{hkl} = \frac{kt}{t} + 4\varepsilon.\sin\theta_{hkl}} \quad \textbf{(iv)}$$

The above equation represents the uniform strain model (USM) of Williamson-Hall analysis (W-H analysis) in which strain distribution is isotropic throughout the crystal. The magnitude of strain and size can be estimated by the slope and the intercept of the graph plotted between '$\beta_{hkl}\cos\theta_{hkl}$' and '$4\sin\theta_{hkl}$' respectively. Since many of the cases of nanomaterials do not fulfill the condition of strain homogeneity. Stress homogeneity and Strain energy homogeneity comes into consideration which is more realistic and logical route [9]. W-H analysis suggested the following models:

A. Uniform Stress Deformation Model (USDM):

$$\beta_{hkl}\cos\theta_{hkl} = \frac{k\lambda}{t} + \frac{4\sigma\sin\theta_{hkl}}{E_{hkl}} \quad \textbf{(v)}$$

B. Uniform Strain Energy Density Model (USEDM):

$$\beta_{hkl}\cos\theta_{hkl} = \frac{k\lambda}{t} + 4\sin\theta_{hkl}\left(\frac{2u}{E_{hkl}}\right)^{\frac{1}{2}} \quad \textbf{(vi)}$$

For the cubic system,

$\boldsymbol{E_{hkl}}^{-1} = \boldsymbol{S_{11}} - 2\left(\boldsymbol{S_{11}} - \boldsymbol{S_{12}} - \frac{\boldsymbol{S_{44}}}{2}\right)(\boldsymbol{l^2m^2} + \boldsymbol{m^2n^2} + \boldsymbol{n^2l^2})$ [10] was used as elastic moduli for the plane (hkl), where $\mathbf{S_{11}}$ = **1.7826×10^{-3} GPa^{-1},** $\mathbf{S_{12}}$ = **-0.3913×10^{-3} GPa^{-1} and** $\mathbf{S_{44}}$ = **7.1428×10^{-3} GPa^{-1}**[11]. In model (A), the anisotropic micro-strain is induced by the isotropic stress while in the case of (B), isotropic deformation energy density causes the anisotropic deformation.

According to Hook's law, $\boldsymbol{\sigma} = \boldsymbol{\varepsilon}.\boldsymbol{E_{hkl}}$ and $\boldsymbol{u} = \frac{\boldsymbol{\varepsilon^2 E_{hkl}}}{\mathbf{2}}$ are being used to calculate the strain and strain energy density respectively as shown in figure 11-19 for different samples synthesized at different conditions. The dependency of β_{hkl} on tanθ instead of $(\cos\theta)^{-1}$ allows the separation of diffracted beams when crystallite size and strain involve into system simultaneously [12].

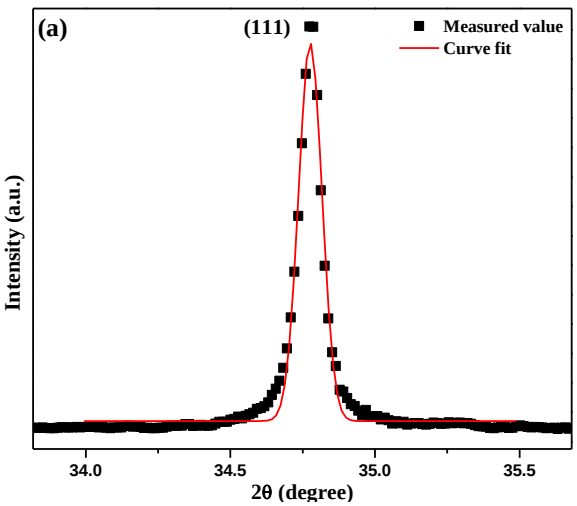

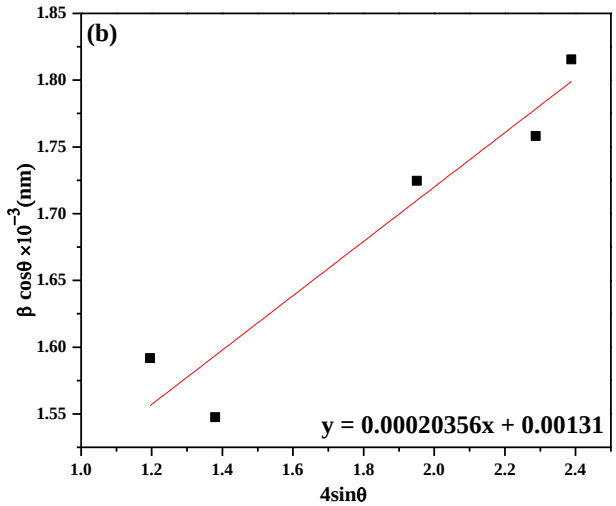

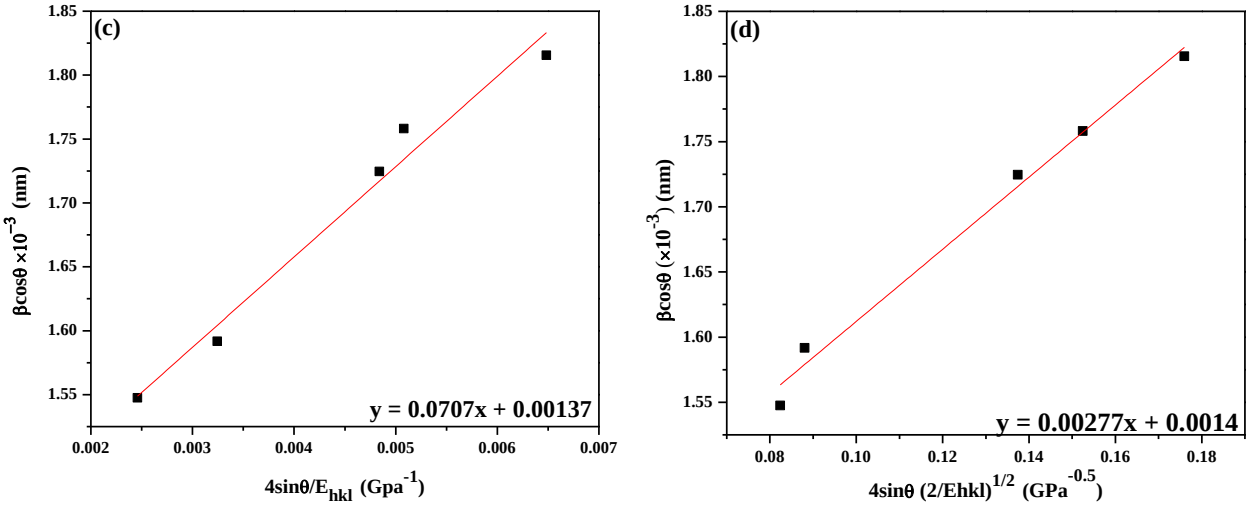

Figure 11: The W-H analysis of the sample '1N600 2.5', the crystalline size is extracted from the y-intercept of the fit. The strain, stress and deformation strain energy density is extracted from the slope (a) Gaussian fitted data, (b) USM, (c) USDM and (d) USEDM.

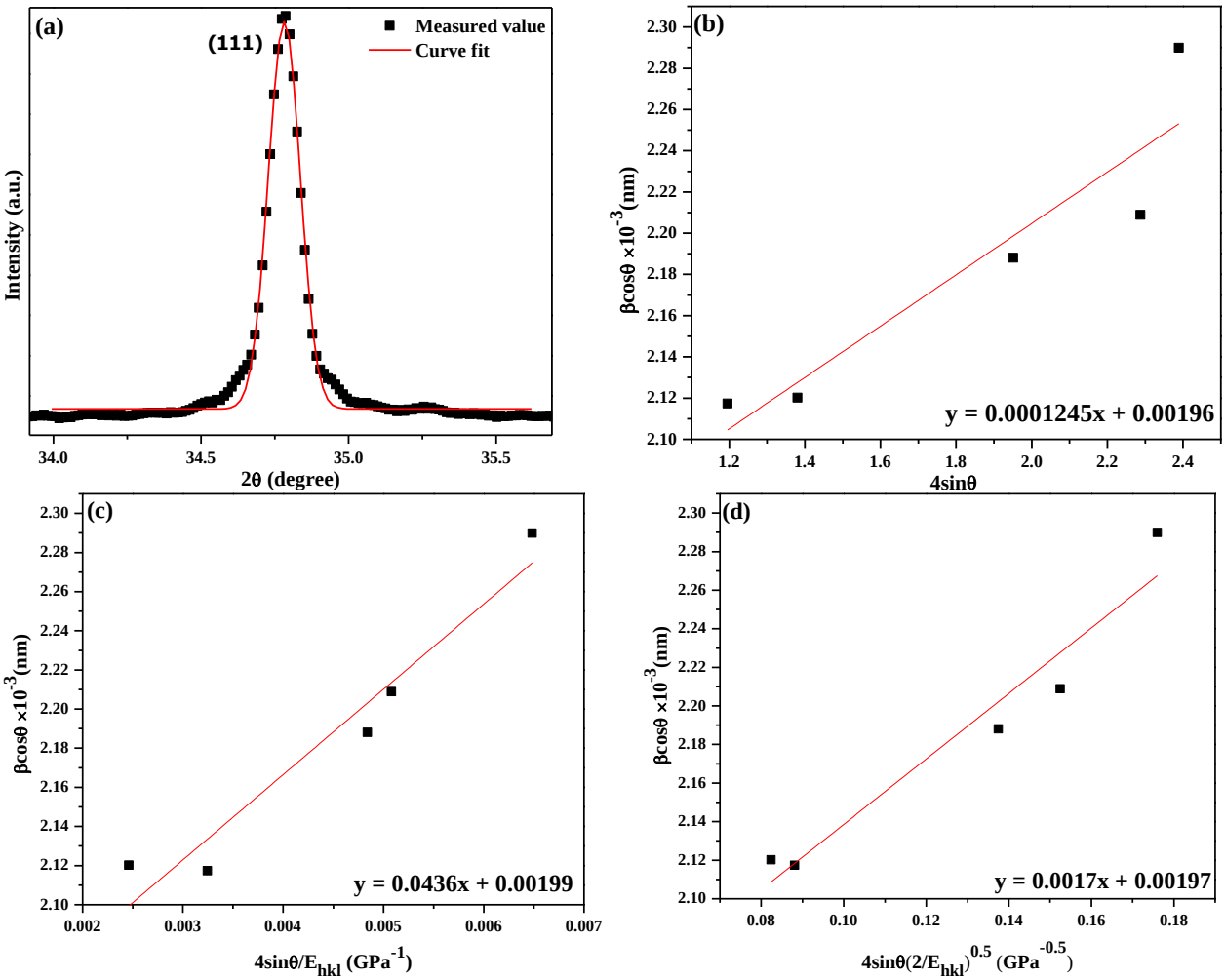

Figure 12: The W-H analysis of the sample '1N600', the crystalline size is extracted from the y-intercept of the fit. The strain, stress and deformation strain energy density is extracted from the slope (a) Gaussian fitted data, (b) USM, (c) USDM and (d) USEDM.

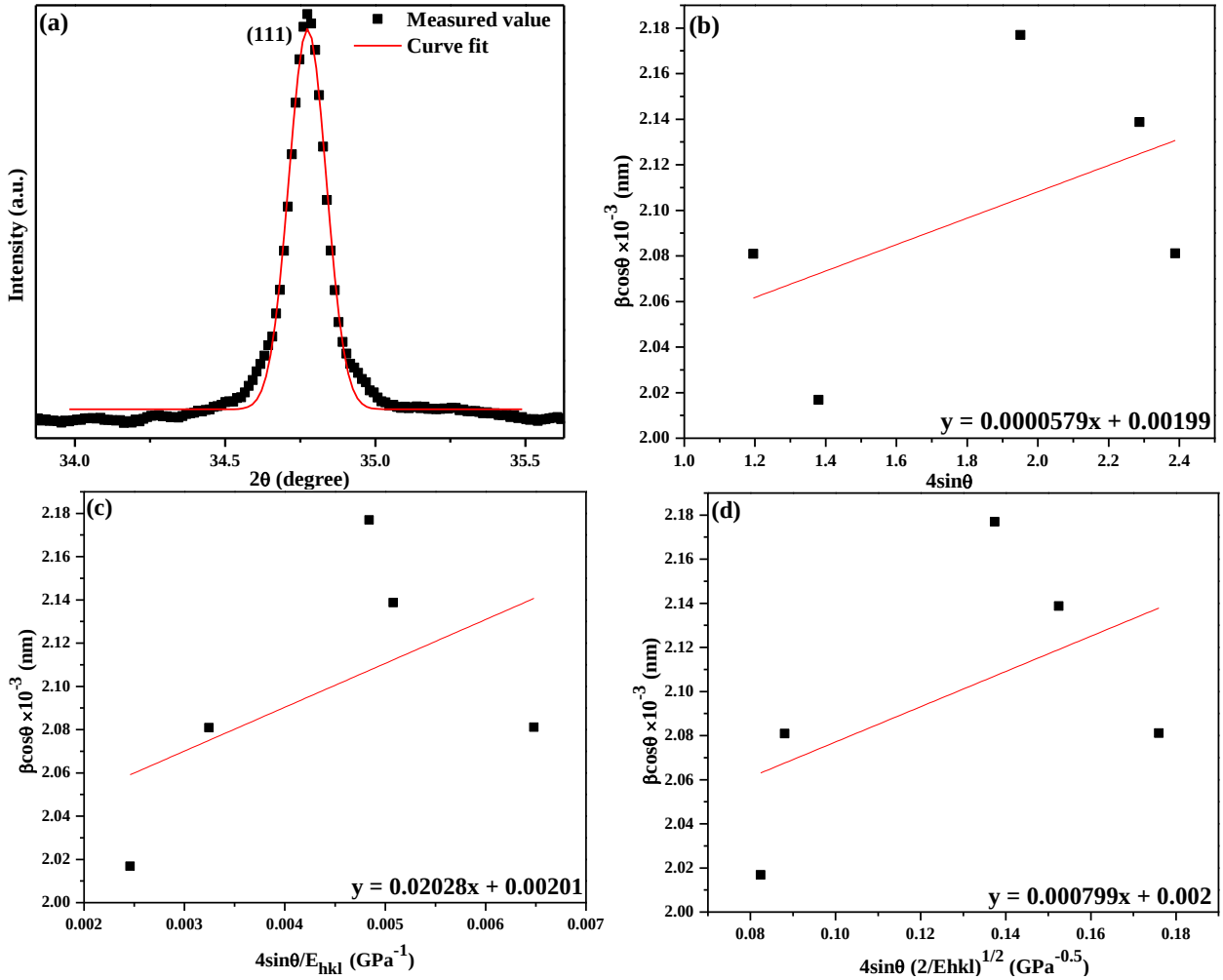

Figure 12: The W-H analysis of the sample '1N600 7.5', the crystalline size is extracted from the y-intercept of the fit. The strain, stress and deformation strain energy density is extracted from the slope (a) Gaussian fitted data, (b) USM, (c) USDM and (d) USEDM.

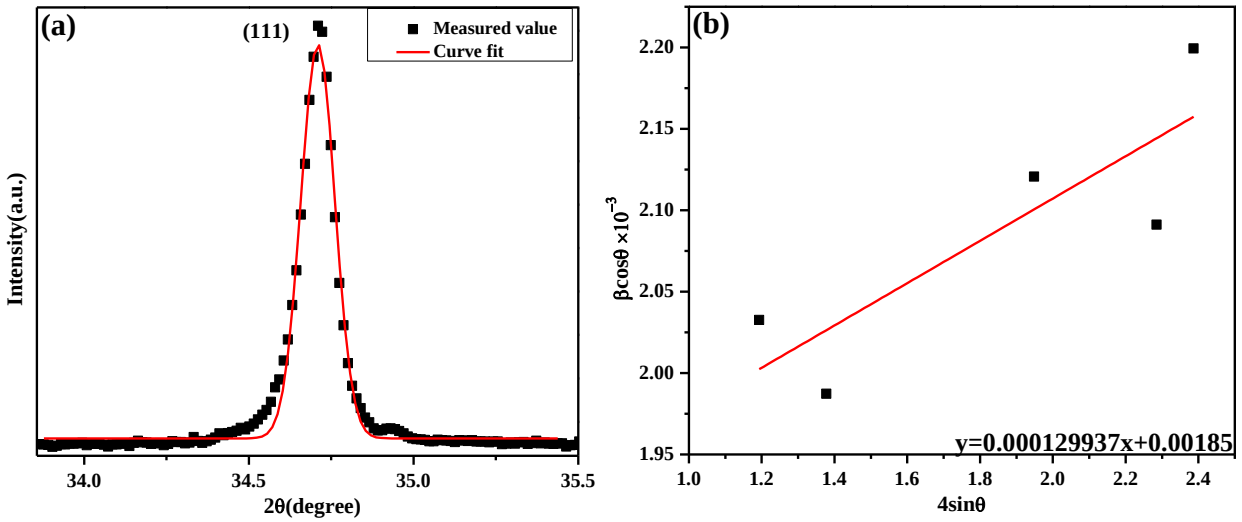

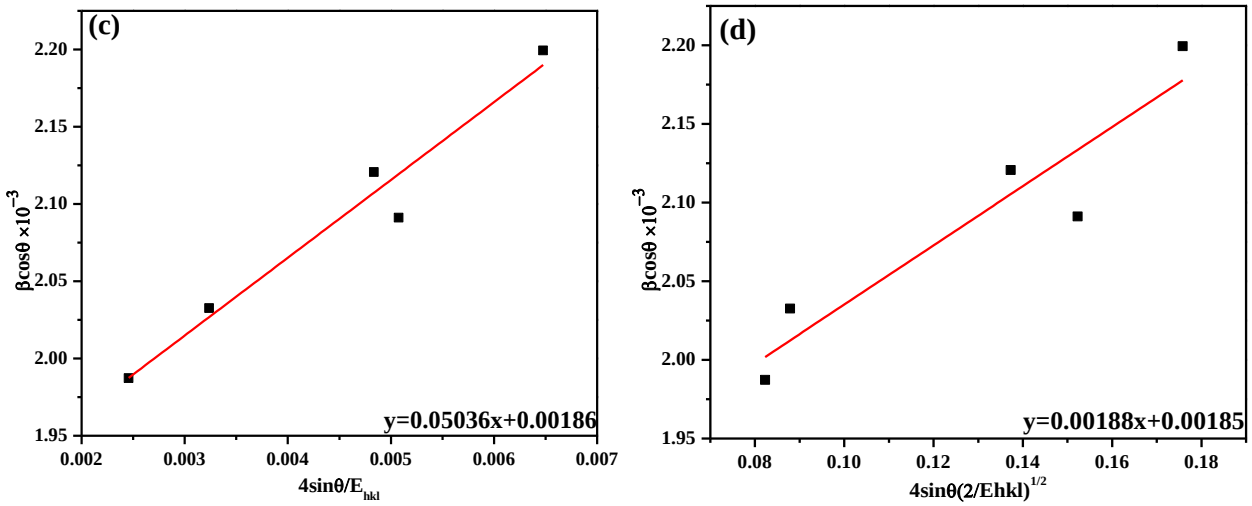

Figure 14: The W-H analysis of the sample '2N600', the crystalline size is extracted from the y-intercept of the fit. The strain, stress and deformation strain energy density is extracted from the slope (a) Gaussian fitted data, (b) USM, (c) USDM and (d) USEDM.

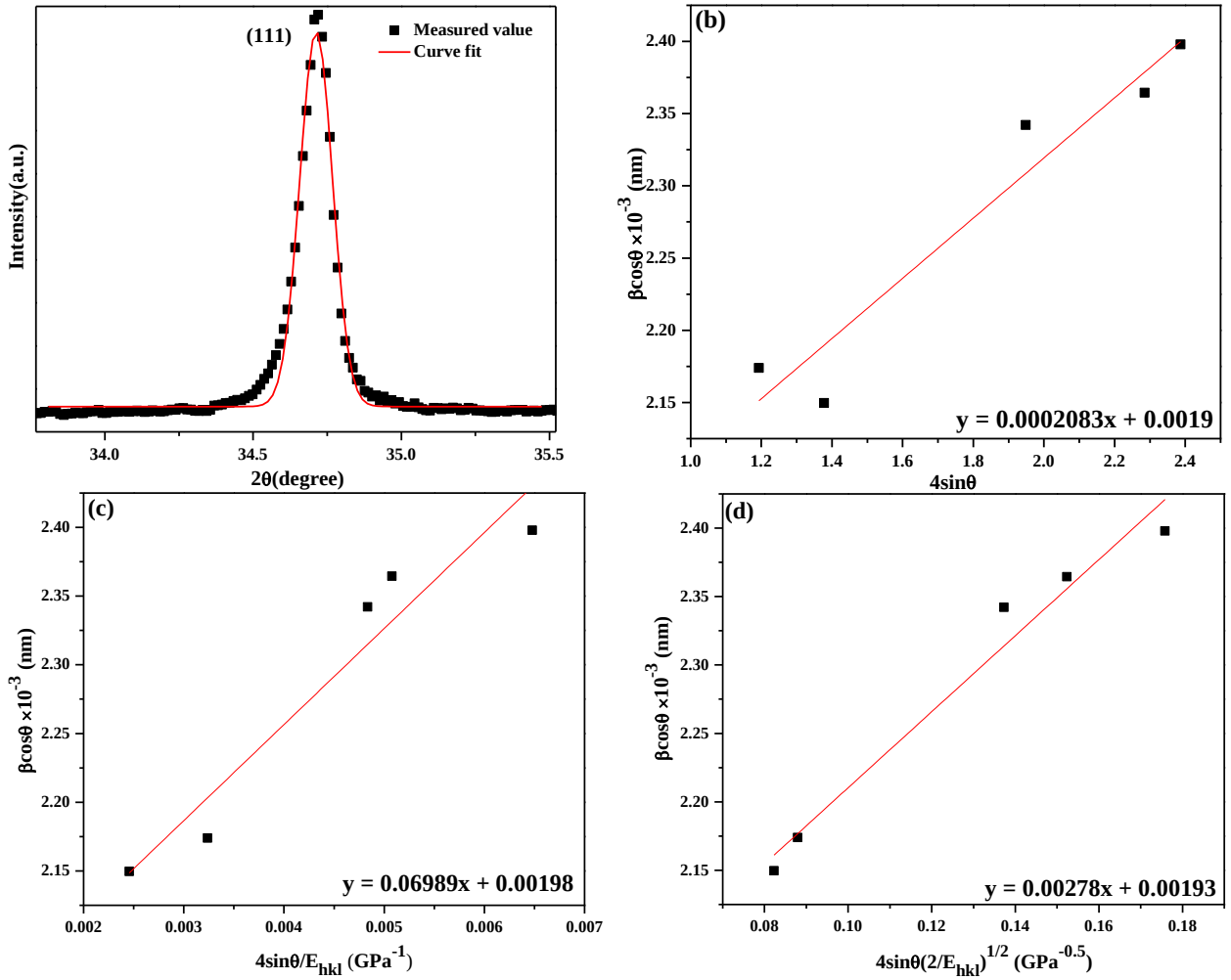

Figure 15: The W-H analysis of the sample '5N600', the crystalline size is extracted from the y-intercept of the fit. The strain, stress and deformation strain energy density is extracted from the slope (a) Gaussian fitted data, (b) USM, (c) USDM and (d) USEDM.

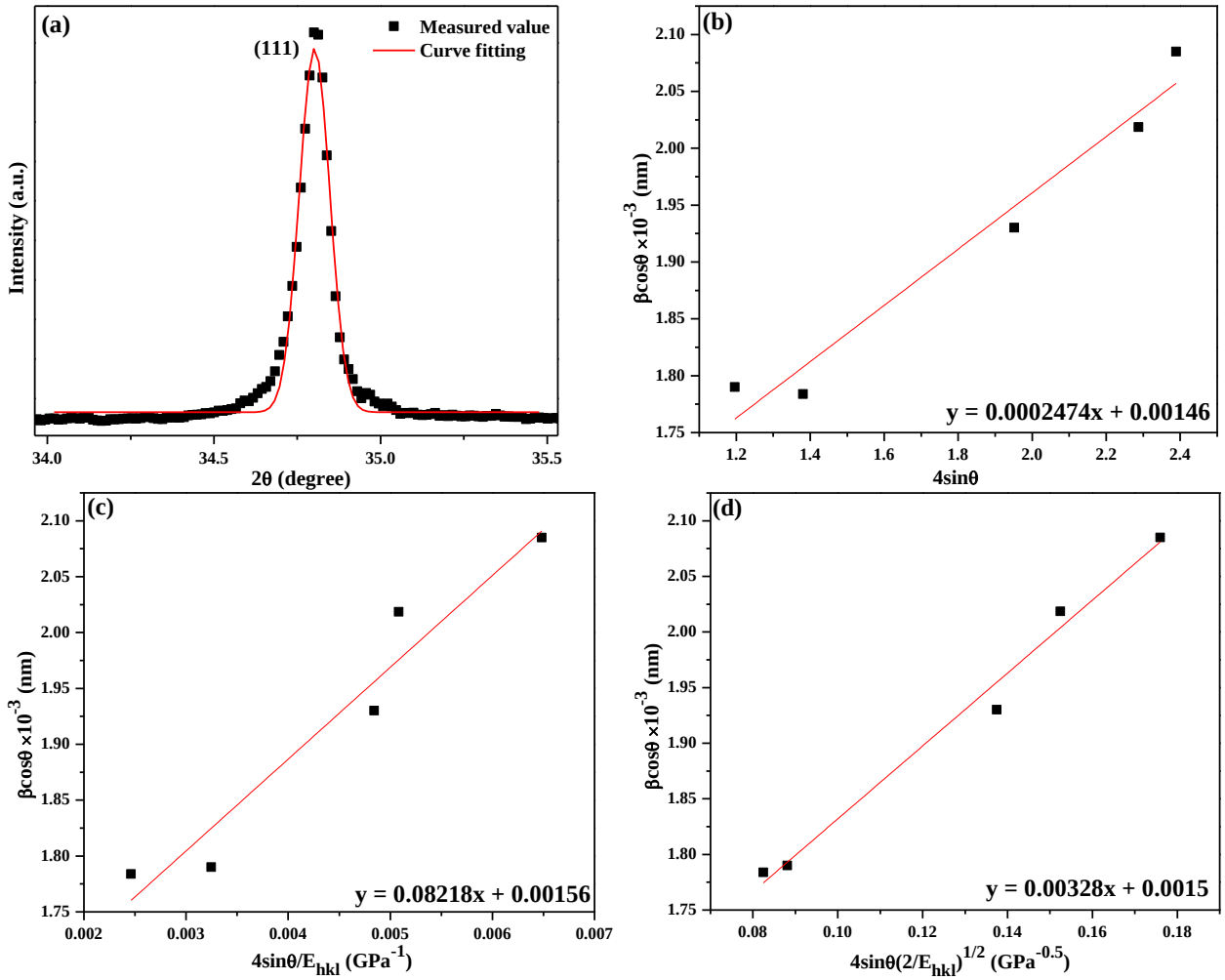

Figure 16: The W-H analysis of the sample '7N600', the crystalline size is extracted from the y-intercept of the fit. The strain, stress and deformation strain energy density is extracted from the slope (a) Gaussian fitted data, (b) USM, (c) USDM and (d) USEDM.

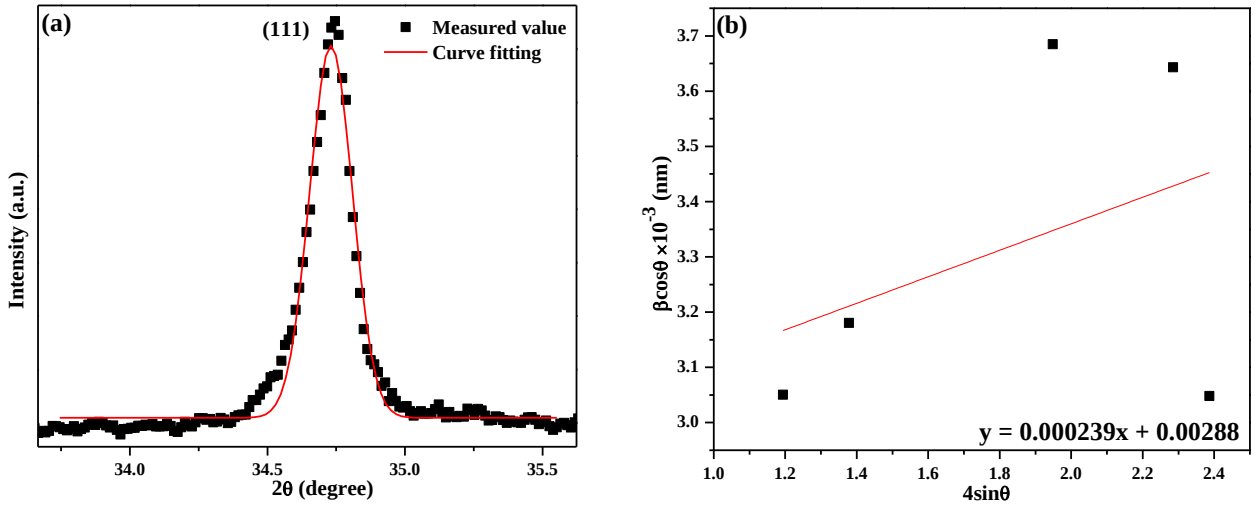

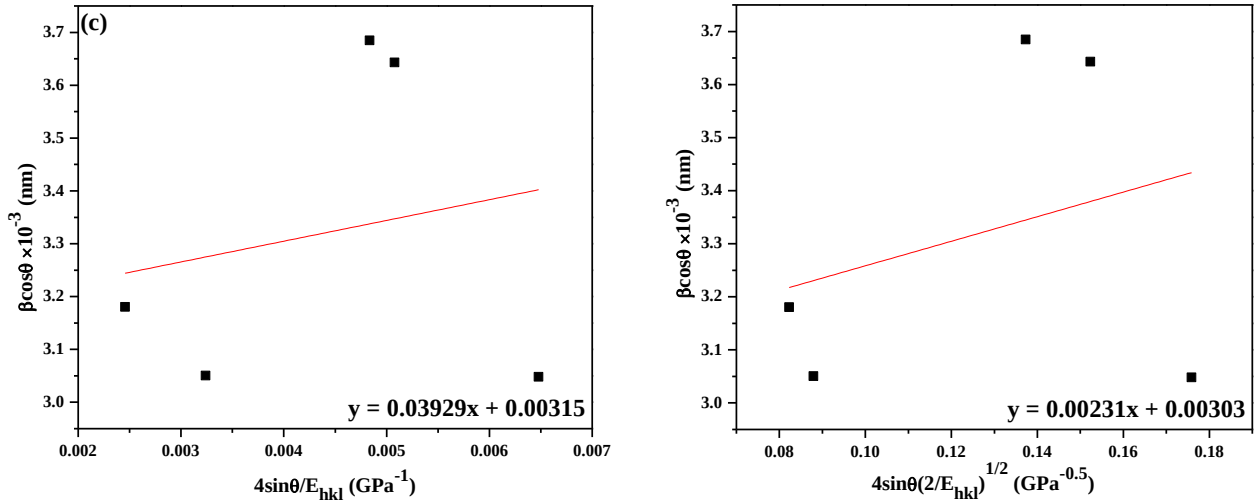

Figure 17: The W-H analysis of the sample '10N600', the crystalline size is extracted from the y-intercept of the fit. The strain, stress and deformation strain energy density is extracted from the slope (a) Gaussian fitted data, (b) USM, (c) USDM and (d) USEDM.

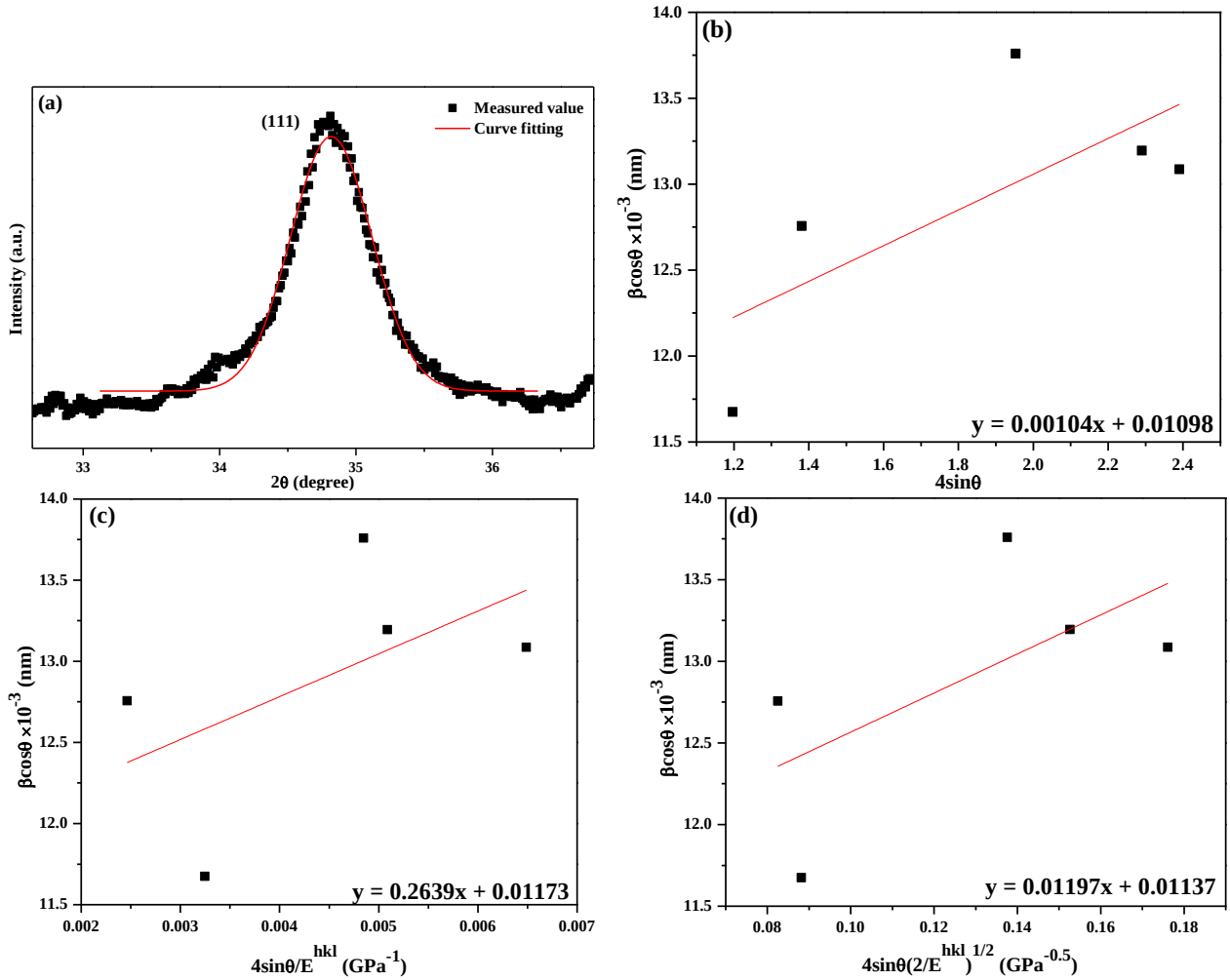

Figure 18: The W-H analysis of the sample '10C700', the crystalline size is extracted from the y-intercept of the fit. The strain, stress and deformation strain energy density is extracted from the slope (a) Gaussian fitted data, (b) USM, (c) USDM and (d) USEDM.

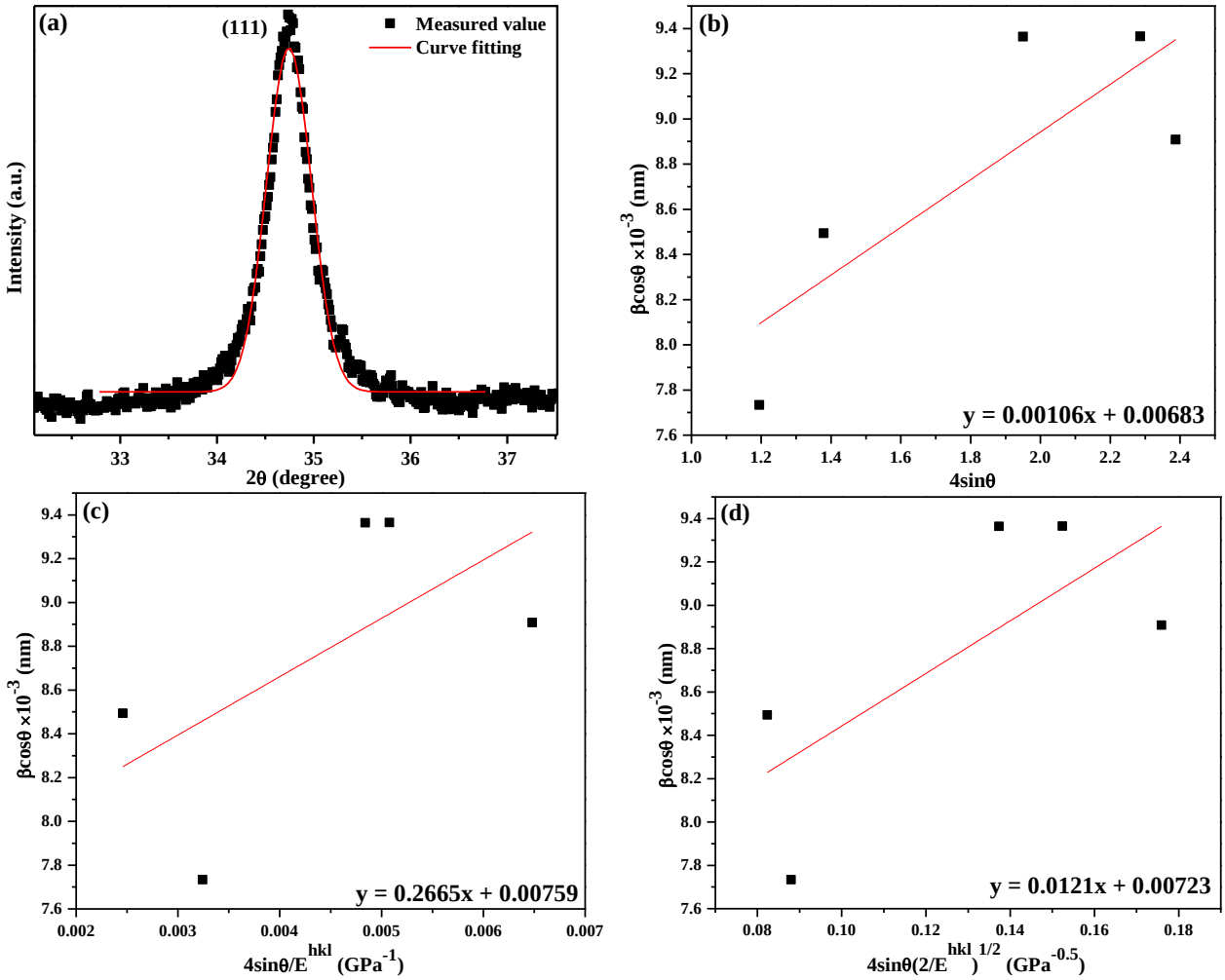

Figure 19: The W-H analysis of the sample '10C800', the crystalline size is extracted from the y-intercept of the fit. The strain, stress and deformation strain energy density is extracted from the slope (a) Gaussian fitted data, (b) USM, (c) USDM and (d) USEDM.

Table 6: Williamson-Hall analysis of all synthesized samples.

Sample Id	USM		USDM			USEDM				Scherrer Method, t (nm)
	ε ×10^{-4}	t nm	ε ×10^{-4}	σ GPa	t nm	ε ×10^{-4}	σ GPa	u ×10^{-5} kJm^{-3}	t nm	
1N6002.5	2.035	117.3	1.684	0.071	112.0	1.905	0.081	0.766	115.3	91.63
1N600	1.245	78.7	1.038	0.043	77.3	1.168	0.049	0.029	78.2	70.57
1N600 7.5	0.579	77.3	0.483	0.020	76.6	0.550	0.023	0.064	77.1	73.45
2N600	1.299	83.3	1.199	0.050	82.6	1.294	0.055	0.354	83.4	86.58
5N600	2.083	80.9	1.665	0.069	77.9	1.912	0.081	0.772	79.7	81.95
7N600	2.474	105.1	1.925	0.082	98.8	2.255	0.095	1.074	102.4	80.49
10N600	2.398	53.4	0.936	0.039	48.9	1.593	0.067	0.536	50.8	50.84
10C700	10.39	14.0	6.289	0.264	13.1	0.403	0.017	14.33	13.5	11.98
10C800	10.55	22.5	6.351	0.266	20.2	8.352	0.355	14.72	21.3	17.65

Various calculated postulates of Williamson-Hall analysis are enlisted in table 6 from which, it is very much elucidated that as we increase the impregnation duration at 600 °C, the amount of induced strain in the crystal lattice keeps on increasing to its highest value 1.294×10^{-4} at 7 h (sample '7N600') impregnation. There is lesser difference in induced strain in 1h and 2h impregnation as compared to other 5 h and 7 h impregnation due to the less amount of NbO_2 at lower impregnation. Least impregnation of 1h at 5 ºC/min leads to the smallest crystallite size i.e. 78.2 nm while slowest heating (2.5 ºC/min) results in the higher growth of crystallite (115.3 nm) which suggested the proper homogenization of energy to promote the growth of crystal.

The broadening of XRD pattern of samples '10C800' and '10C700' is supported by W-H analysis which suggested smaller crystallite size (~13 and ~20 nm) and huge amount of strain contained in crystallite (figure 10 & table 6). While 2N600, 5N600 possess sharp peaks correspond to larger crystallite with less strained particle (figure 7 & table 6).The mechanism behind the carbo-reduction of Nb_2O_5 to form NbC by escaping oxygen to add carbon in niobium crystal is shown as follows (fig. 20):

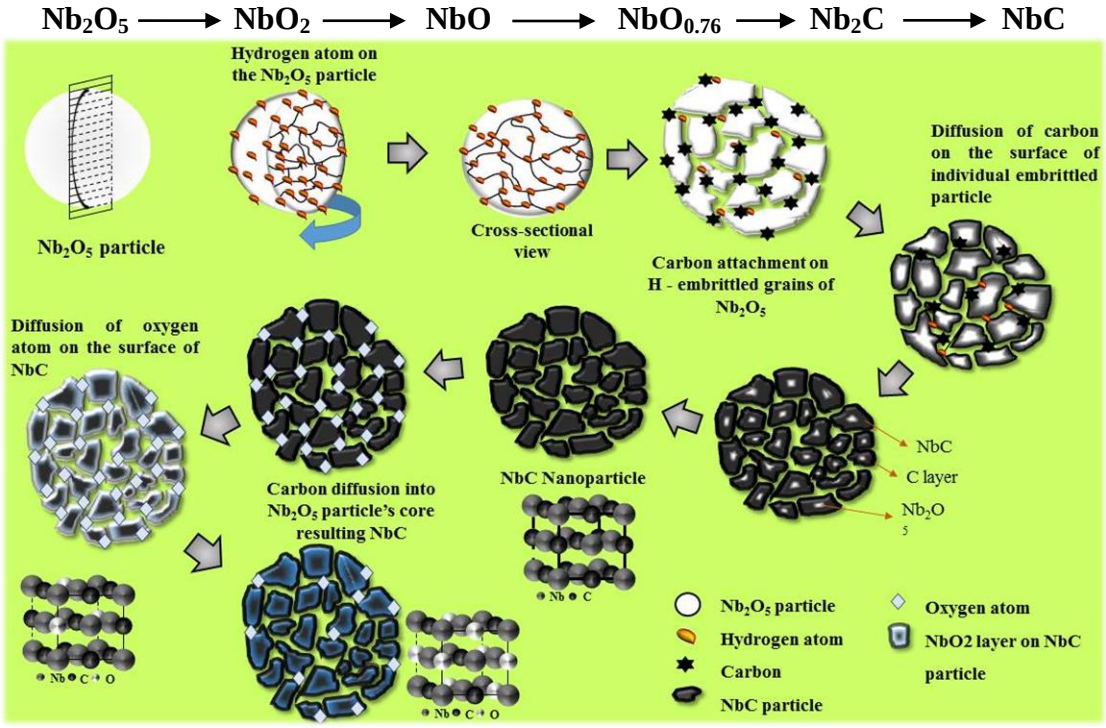

Figure 20: Mechanism of reduction-carburization of Nb_2O_5 to form NbC.

4.3. Thermal Analysis:

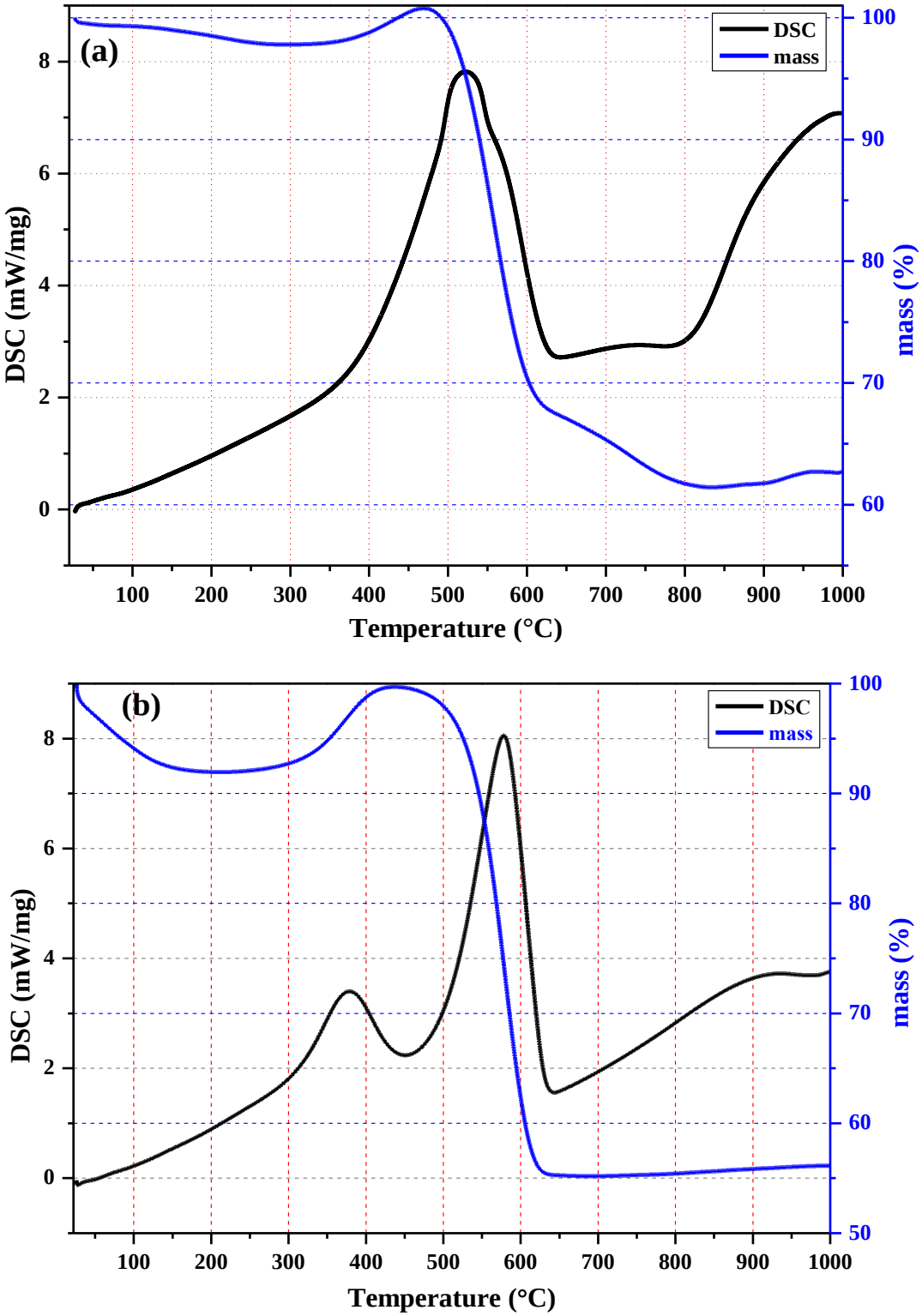

Figure 21: DSC/TGA study of (a) 2N600 and (b) 10C700.

Figure 21 shows the thermal behavior of '2N600' and '10C700' through DSC/TGA study in the presence of air with heating rate of 5ºC/min. TGA pattern of '2N600' (fig. 21a) shows a little

weight loss (~2.2%) upto 330ºC which may be associated with the removal of adsorbed water molecules on the surface of the synthesized NbC. In region 350-470ºC, around 3.8% weight gain is observed which corresponds to the oxidation of NbC particle [13]. Beyond 470ºC, huge mass loss occurred which continued to 820ºC. This region of thermo-gravimetric curve suggested the combined effect of oxidation of carbon and NbC particle, resulted into the weight loss of 39% [14, 15]. From 620 ºC to 840 ºC, the rate of mass loss is slowed down due to the formation of oxide layer on the NbC particles at lower temperature which hinders the further oxidation and decarburization [2]. Further increase in temperature lead to form Nb oxide at very slower rate upto 1000ºC which indicates the tendency of diffusion of oxygen at high temperature to attain more stable phase configuration.

When carbon source is changed to charcoal (10C700), the particle size of NbC has reduced which can be observed from XRD patterns. In thermal study (fig. 21b), due to that smaller size (higher surface area), significant mass loss (~8%) is obtained below 300ºC corresponding to extensive water loss and carbonaceous content. Theoretically removal of vapor associates 14.75% mass loss but experimentally it cannot be occurred due to the simultaneous oxidation of undetectable Nb metal and amorphous carbon present on the NbC particle [13]. Because of oxidation of Nb metal (17.39% mass gain) slight mass gain is observed between 300 and 440ºC. Further huge mass loss (~45%) is endured between 500 and 640ºC corresponding to combined oxidation of carbon layer and NbC. Upto this temperature the synthesized NbC nano particle of size 12nm shows good stability against temperature. Beyond 632ºC, TG curve stabilizes and shows very slow rate of oxidation which suggests only 1.2% weight gain upto 1000ºC.

Sample ‘10C700’ shows poor thermal stability as compared to ‘2N600’ because of the presence of dual phases i.e. NbC and Nb_2C and higher surface area. Dual phases cause more strain energy content within the lattice and shifts the mass loss peak by 27ºC to lower temperature which is also supported by Williamson-Hall analysis of these samples.

4.4. Microstructural analysis:

The SEM analysis of the sample '2N 600' shows that NbC particles have very high tendency to agglomerate and there is huge bunch of particles as shown in figure 22a. TEM analysis of the same sample shows the particle size about 90 nm which is nearly similar to the calculated data from Williamson-Hall and Scherrer methods. From the TEM micrograph of 2N600, it is clear that growth of NbC particle is partially smooth and partially faceted (fig. 22b) and there is a transparent layer of carbon on the NbC particle. Figure 23 shows the lattice fringes of plane (200) of NbC crystal observed under HR-TEM analysis. The carbon layer on NbC particles is amorphous in nature which is confirmed at higher magnification and the NbC particle is crystalline and the inter-planar spacing of respective planes is 0.224 nm which is also supported by XRD fitting data. TEM analysis of '10C800' is shown in figure 24 which suggested the spherical morphology of NbC particle with carbon layer on top of it. HR-TEM micrograph of this sample shows the lattice fringes corresponding to plane (111) with spacing of 0.262 nm as shown in figure. TEM analysis of both the samples suggested the systematic reduction of oxide particle (concentric circular pattern in particle) and the core-shell structure of synthesized NbC nano particles [16] in which interface is not distinct suggesting its transient nature.

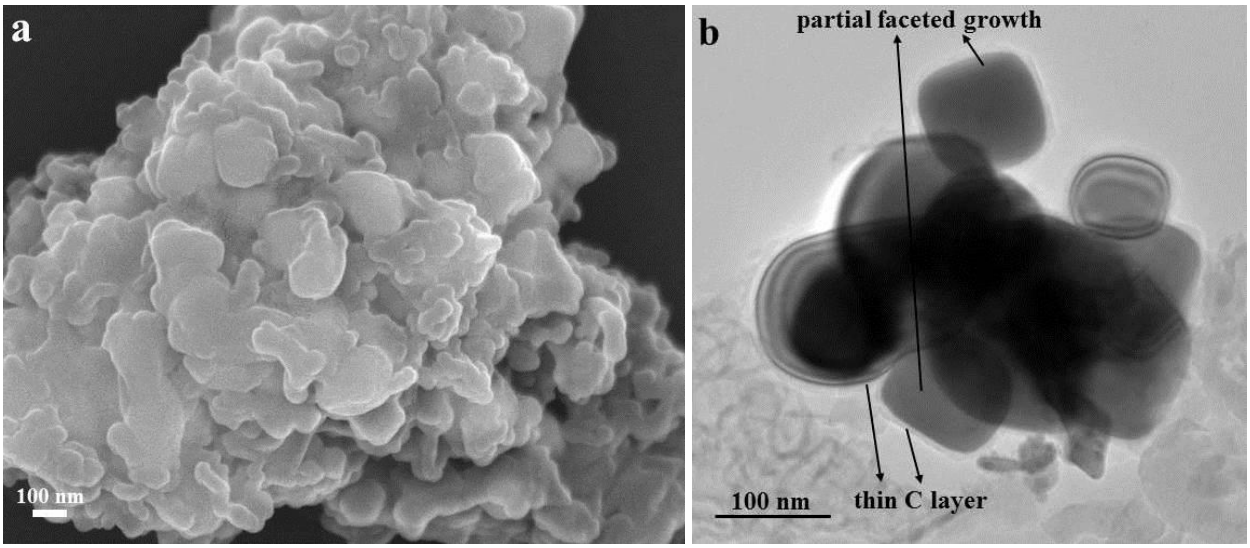

Figure 22: (a) SEM micrograph shows various morphological features of sample '2N600', (b) TEM micrograph of 2N600 suggesting the faceted and non-faceted morphology.

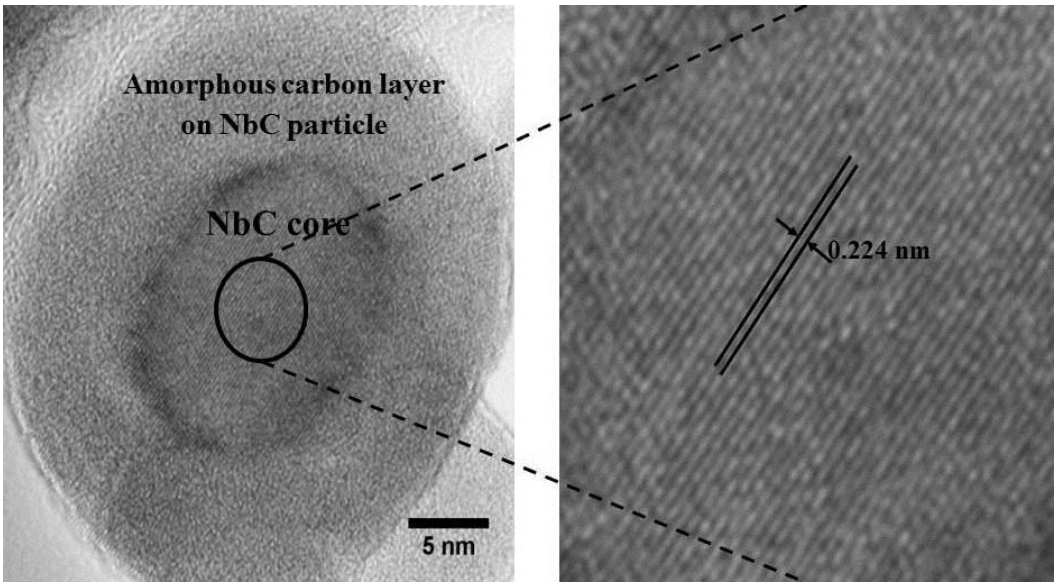

Figure 23: TEM micrograph of sample '2N600' indicating the carbon layer on NbC's particle with its amorphous nature, lattice fringes of plane (200) of cubic NbC.

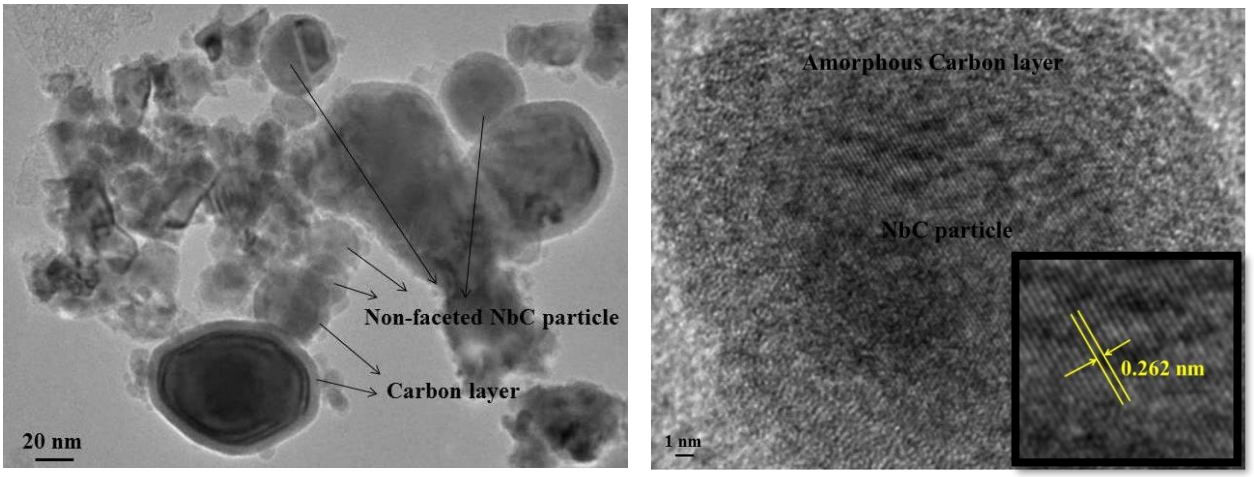

Figure 24: TEM micrograph of sample '10C800' indicating the carbon layer on NbC's particle with its amorphous nature, lattice fringes of plane (111) of cubic NbC.

4.5. References:

[1] L. Shi, Y. Gu, L. Chen, Z. Yang, J. Ma and Y. Qian, **Synthesis and oxidation behavior of nanocrystalline niobium carbide,** Solid State Ionics 176, 841 (2005).

[2] A.S. Shevchenko, R.A. Lyutikov, R.A. Andrievskii and V.A. Terekhova, **Oxidation of zirconium and niobium carbides**, Soviet Pow. Met. and Metal Cer. 19(1), 48 (1980).

[3] T.Y. Kosolapova, **Carbides: properties, production and applications**, Plenum Press, NewYork-London (1971).

[4] F.A.O. Fontes, K.K.P. Gomes, S.A. Oliveira, C.P. Souza and J.F. Sousa, **Niobium carbide synthesis by solid-gas reaction using a rotating cylinder reactor,** Braz. J. of Chem. Eng. 21(3), 393 (2004).

[5] J.O. Hill, I.G. Worsley and L.G. Hepler, **Thermochemistry and oxidation potentials of vanadium, niobium and tantalum**, Chemical Reviews 71(1), 127 (1971).

[6] H. Kwon, W. Kim and J. Kim, **Stability domains of NbC and Nb(CN) during carbothermal reduction of niobium oxide**, J. of Am. Cer. Soc. 98(1), 315 (2015).

[7] F.O. Rice and R.E. Vollrath, **The thermal decomposition of acetone in gaseous state**, Proc. Natl. Acad. USA 15(9), 702 (1929).

[8] S. Vives, E. Gaffet and C. Meunier, **X-ray diffraction line profile analysis of iron ball milled powders,** Mat. Sci. and Eng. A(366), 229 (2004).

[9] G. Singla, K. Singh and O.P. Pandey, **Willianson-Hall study on synthesized nanocrystalline tungsten carbide (WC)**, Applied Physics A (113), 237 (2013).

[10] E.A. Brands and G.B. Brook, **Smithells metas reference book**, 7th Edition, Butterworth-Heinemann (1999) 1088: ISBN 0-7506-3624-6.

[11] J. Chen, L.L. Boyer, H. Krakauer and M.J. Mehl, **Elastic constants of NbC and MoN: instability of B_1-MoN**, Phys. Rev. B 37(7), 3295 (1988).

[12] A. K. Zak, W.H. Abd. Majid, M.E. Abrishami and Ramin Yousefi, **X-ray analysis of ZnO nanoparticles by Williamson-Hall and size-strain plot methods**, Solid State Sciences 13(1), 251 (2011).

[13] L.K. Brar, G. Singla, N. Kaur and O.P. Pandey, **Thermal stability and structural properties of a nanopowder synthesized via simultaneous reduction of Ta_2O_5 by hydrogen and carbon**, J. Thermal Anal. Calorim. 119, 175 (2015).

[14] S. Shimada and M. Inagaki, **A kinetic study on oxidation of niobium carbide**, Solid State Ionics, 312 (1993).

[15] Z.Q. Li, H-F. Zhang, X.B. Zhang, Y.Q. Wang and X J. WU, **Nanocrystalline tungsten carbide encapsulated in carbon shells**, Nanostructured Materials 10(2), 179 (1998).

[16] M. Mahajan, N.P. Lalla, K. Singh and O.P. Pandey, **Synthesis and photoluminescence properties of in-situ synthesized core shell (m-VC@C) nanocomposites,** Materials Chemistry and Physics 160, 48 (2015).

5. Conclusion:

Core-shell NbC nanopowder has been synthesized successfully via single step carbo-thermal route using niobium oxide as niobium source and acetone and charcoal as carbon source. Among all the synthesis configurations, 2 hours impregnation time at 600 ºC provides the maximum carbon content in the niobium crystal i.e. 0.991 which is nearly stoichiometric composition. That implies the almost all the octahedral voids are filled by the carbon atom which lead to the most stable configuration. It is very much elaborated that the morphological features of NbC nano particles are quite different when charcoal is used to synthesize NbC. Almost 17 nm (diameter) sized particles are synthesized with charcoal which is quite smaller as compared to the particles that are synthesized with acetone (~83 nm). This feature may lead to higher surface area. Moreover, the thermal analysis of this sample shows that NbC nano powder is stable upto 470 ºC. The coated amorphous carbon endorsed the stability of NbC severe chemical environments. The influence of heating rate is also observed in the synthesized samples, which gives maximum content of NbC at lower heating rate (2.5 °C/min). The microstructural study confirms the formation of carbon encapsulated NbC nano particle which designates core-shell morphology.

6. Future scope:

The synthesized NbC at nano scale can be used as reinforcement in aluminum alloys to enhance its mechanical properties such as strength, hardness, wear behavior and specially damping characteristics so that it can be used in aeronautical applications. The synthesized NbC powder can further be used for its electrochemical study to see the feasibility of its suitable use as catalyst for different types of electrochemical applications.